MAGNETICS OF BOWIE SEAMOUNT

by

RONALD NICK MICHKOFSKY

B.Sc., Carnegie Institute of Technology
(Carnegie-Mellon University), 1967

A THESIS SUBMITTED IN PARTIAL FULFILMENT OF

THE REQUIREMENTS FOR THE DEGREE OF

MASTER OF SCIENCE

in the Department

of

GEOPHYSICS

We accept this thesis as conforming to the
required standard

THE UNIVERSITY OF BRITISH COLUMBIA

April, 1969

In presenting this thesis in partial fulfilment of the requirements for

an advanced degree at the University of British Columbia, I agree that

the Library shall make it freely available for reference and Study.

I further agree that permission for extensive copying of this thesis

for scholarly purposes may be granted by the Head of my Department or

by his representatives. It is understood that copying or publication

of this thesis for financial gain shall not be allowed without my

written permission.

Department of _Geophysics_

The University of British Columbia
Vancouver 8, Canada

Date _May 1, 1969_

ABSTRACT

Using the oceanographic ship, the Endeavor;
the University of British Columbia undertook a study of
Bowie Seamount (53°18', 135°41') during the summer of
1968. Receiving a proton precession magnetometer for
the cruise from PNL, a magnetic field survey was included
in the study. The magnitude of the observed anomaly was
about 850 gammas. The regional was determined by data
taken in an airborne magnetic survey done in 1958 by the
Dominion Observatory. Corresponding to the topography,
the contour plot of the magnetic field showed a strong
linear trend from the SW to the NE. In addition, despite
fairly symmetrical bathymetry, the observed anomaly is
decidedly unsymmetrical, implying a non-uniform intensity
of magnetization. This seems to be confirmed by the use
of a three dimensional model - assuming uniform magneti-
zation - developed by Manik Talwani. Using the least
squares best fit intensity of magnetization, a large dis-
crepancy was found between the model and the observed
anomaly. In light of the fact that the earth's magnetic
field has reversed directions many times in its history,
the above discrepancy may well be due to the fact that
the lava flows of the seamount span at least one time
boundary separating a normal and a reversed magnetic period.
This is given some credence in that an age determination
was made on one sample yielding an age of about 100,000

years, a normal period in the earth's magnetic history. This together with the fact that the magnetic anomaly over most of the seamount is negative yields the above conclusion.

iv

TABLE OF CONTENTS

Page

LIST OF TABLES

LIST OF FIGURES

viii

ACKNOWLEDGEMENTS

CHAPTER I

INTRODUCTION

I-1 Nature of Cruise

In the summer of 1968, the University of British
Columbia undertook a study of Bowie Seamount (53°18'N,
134°41'W). The origin of this cruise was a similar one
that occurred the preceding summer. On that cruise only
echo-sounding and bottom sampling were done. Unfortunately,
the cruise did not adequately accomplish these two tasks.
The reason for this is that the navigation was done by
dead reckoning with respect to a buoy anchored to one of
the shallower (20 to 30 fathoms) parts of the seamount.
Originally, it had been planned to navigate by radar re-
flection, that is a metal reflector was to be attached to
the top of the buoy; however, the rod joining the reflec-
tor to the buoy broke. The resulting poor navigation led
to an inaccurate topographical map.

With the shortcomings of the 1967 cruise, the
1968 one was undertaken. Navigation was accomplished by
means of a radar transponder mounted on an anchored buoy.
With this set up, navigation was good to about .2 of a
mile radially and .5 of a degree azimuthally. Besides
bottom photography and sampling, a bathymetric and a mag-
netic survey were completed.

Data obtained during the cruise is the basis for
the M.Sc. theses of R. Herzer of the Department of Geology

of the University of British Columbia and the author of
this report, R. N. Michkofsky. Mr. Herzer is to inter-
pret the bathymetry, the bottom samples, and the photo-
graphs; I will interpret the magnetic field measurements.

The main instruments used on the cruise are
listed in Table I, along with available model numbers.
Fig. 1 is a schematic of the main deck of the Endeavor,
the oceanographic ship used on the cruise. The ship,
which has a permanent crew of 40, is approximately 250 ft.
in length. The lab's radar was located about 50 ft. above
the water level. Along with the radar transponder and its
corresponding tower, Fig. 2 is a schematic of the buoy
used.

I-2   Proton Precession Magnetometer*

To measure the magnetic field, a Varian Proton
Magnetometer was used. The basic theory of the instrument
is simple. The proton has a precise magnetic moment. On
applying a sufficient field, the magnetic moment tries to
align itself to the applied field. As a consequence, the
proton's axis (direction of the magnetic moment) precesses
about the external field. The frequency of precession is
proportional to the strength of the field, i.e. H (gammas) =

———————————————————

*Varian Associates, Data Sheet

TABLE I

Instruments Used on Cruise

Instrument	Model Number
Edo Echo Sounder (12kH$_z$ Transducer)	185
Alden Precision Graphic Recorder	419
Gift Depth Recorder Transducer (beam width 17°)	
Alpine Geophysical X-Band Radar Transponder	427-D
Decca Radar (Beacon Receiver)	828
Varian Associates Marine Proton Precession Magnetometer	V-4937
E.G. and G. International Camera	205
Light Source	206
Ocean Research Equipment Pinger	250B
Twelve Inch Pipe Dredge	Custom made
Petterson Grab Sampler	Custom made
Dietz-Laford Snapper	

4

STAIRS TO FORE DECK

BOW

CRANE

WINCH FOR GRAB SAMPLING

STAIRS TO SECOND DECK

GANG PLANK

LAB 2

WINCH FOR DREDGING AND CORING

LAB 1

SCALE: .04 IN EQUALS 1 FT.

WINCH FOR MAGNETOMETER

STERN

CRANE
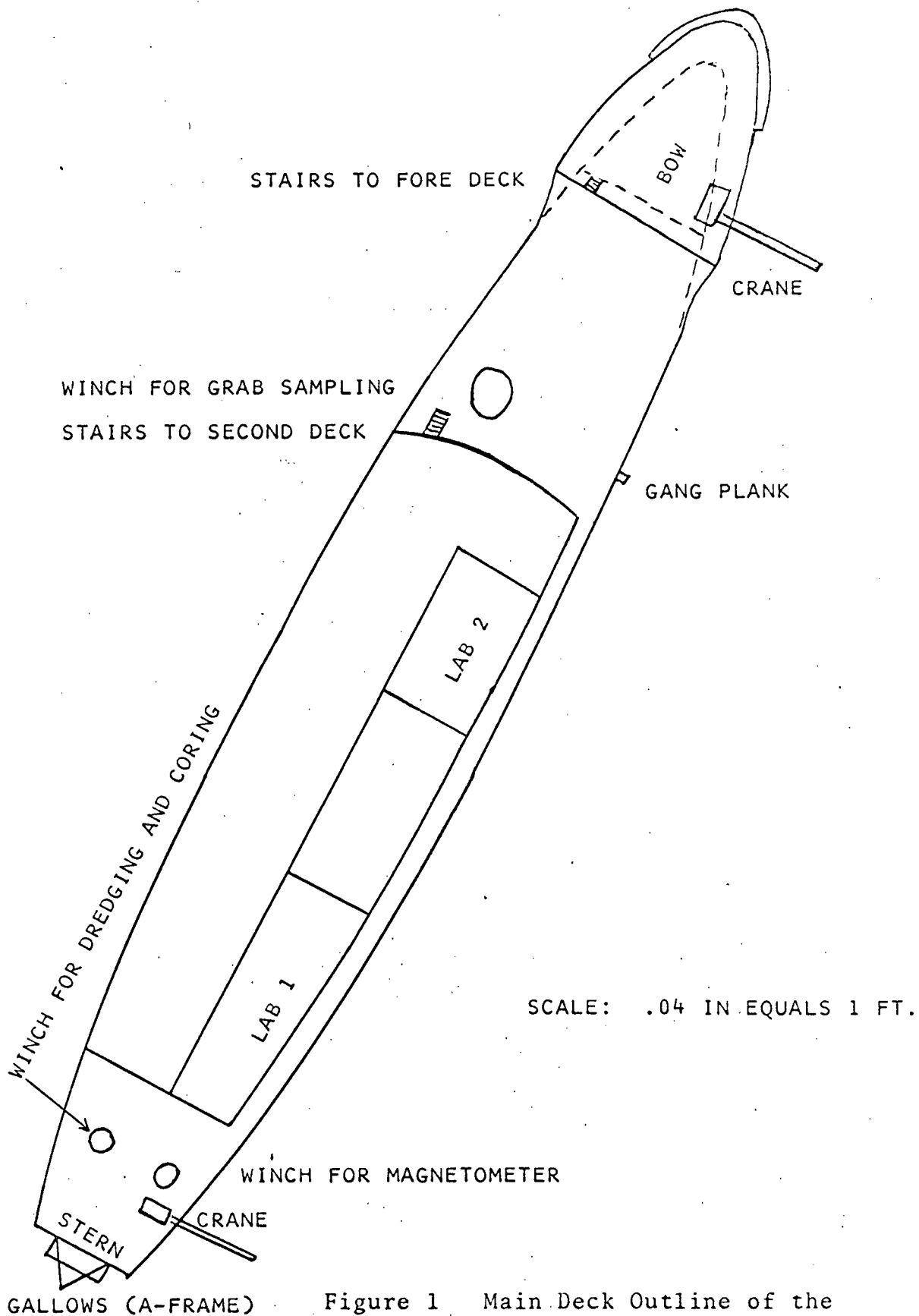
GALLOWS (A-FRAME)   Figure 1   Main Deck Outline of the
                                 Endeavor

RADAR TRANSPONDER

RADAR TRANSPONDER TOWER

AVERAGE WATER LEVEL

BUOY

ANCHOR
(DISCARDED RAILROAD
WHEEL)

SCALE: 1 IN. EQUALS 4 FT.
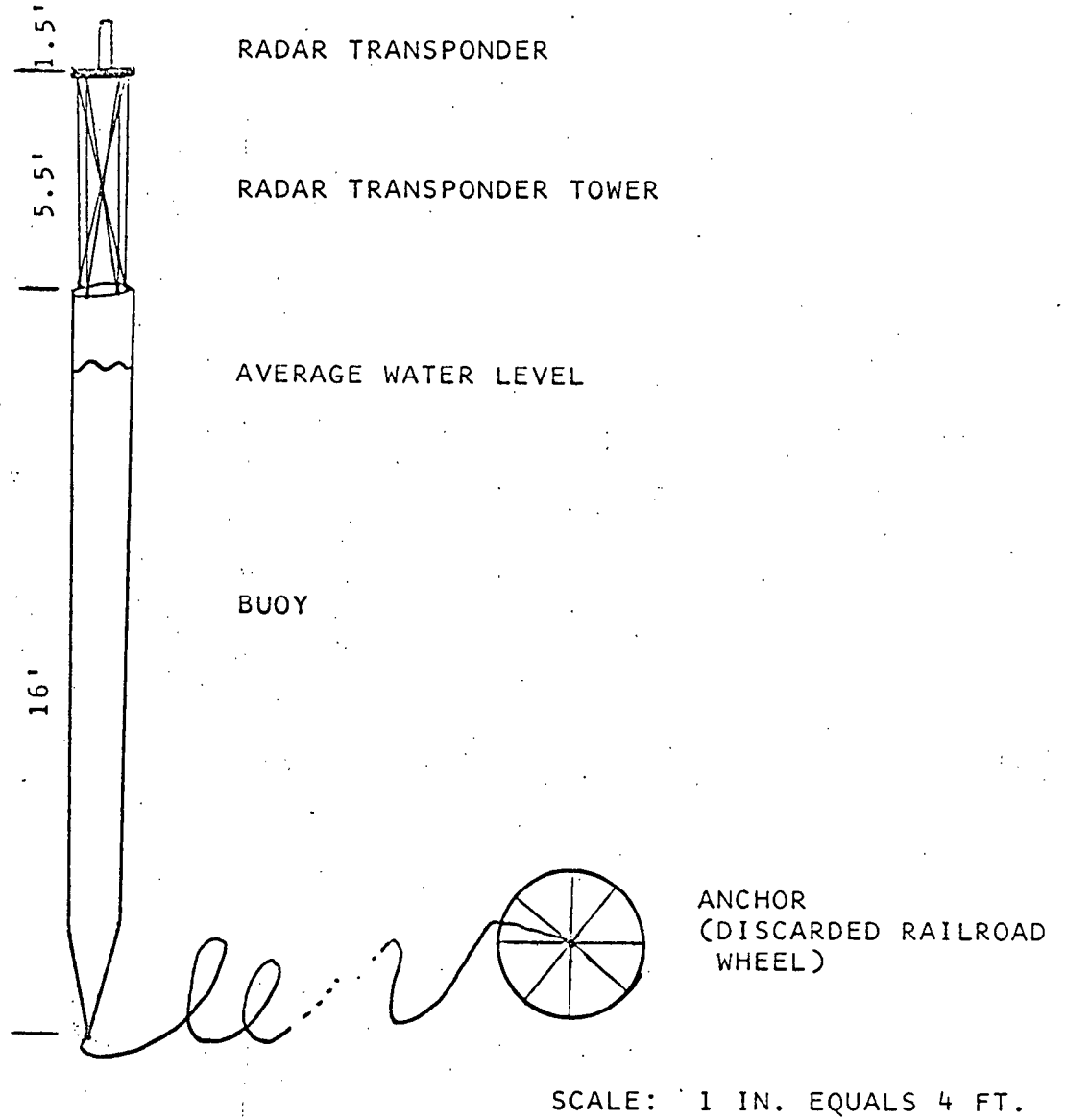
Figure 2   Buoy

23.4875 fp (cycles per second) where fp is the precession frequency. The proton precession magnetometer uses a hydrocarbon fluid to provide a source of protons. By means of a coil that surrounds the fluid, a strong field is applied to the fluid at an angle to the earth's field, causing a polarization of the protons. This field is about two orders of magnitude greater than the earth's magnetic field. The field is cut off and the protons, already orientated, try to align themselves with the earth's field. The precession around the earth's field induces a voltage in the coil at fp . This signal is used to measure the earth's magnetic field. To avoid the possibility of the polarizing field being parallel to the earth's field, two perpendicular coils are used. The induced signal is amplified, is squared, and is entered into a phase detector. The output of the phase detector controls a voltage controlled oscillator which generates a signal about 32 times fp, the precession frequency. To help insure that the output remains at exactly 32 fp, a feed back system is used. A digital frequency counter then counts exactly 23.4875 times fp. A schematic of the above is in Fig. 3. In addition, a few of the instrument's specifications are in Table II. To finish off, I would just like to add that to avoid the magnetic effects of the ship, the sensor head illustrated in Fig. 3
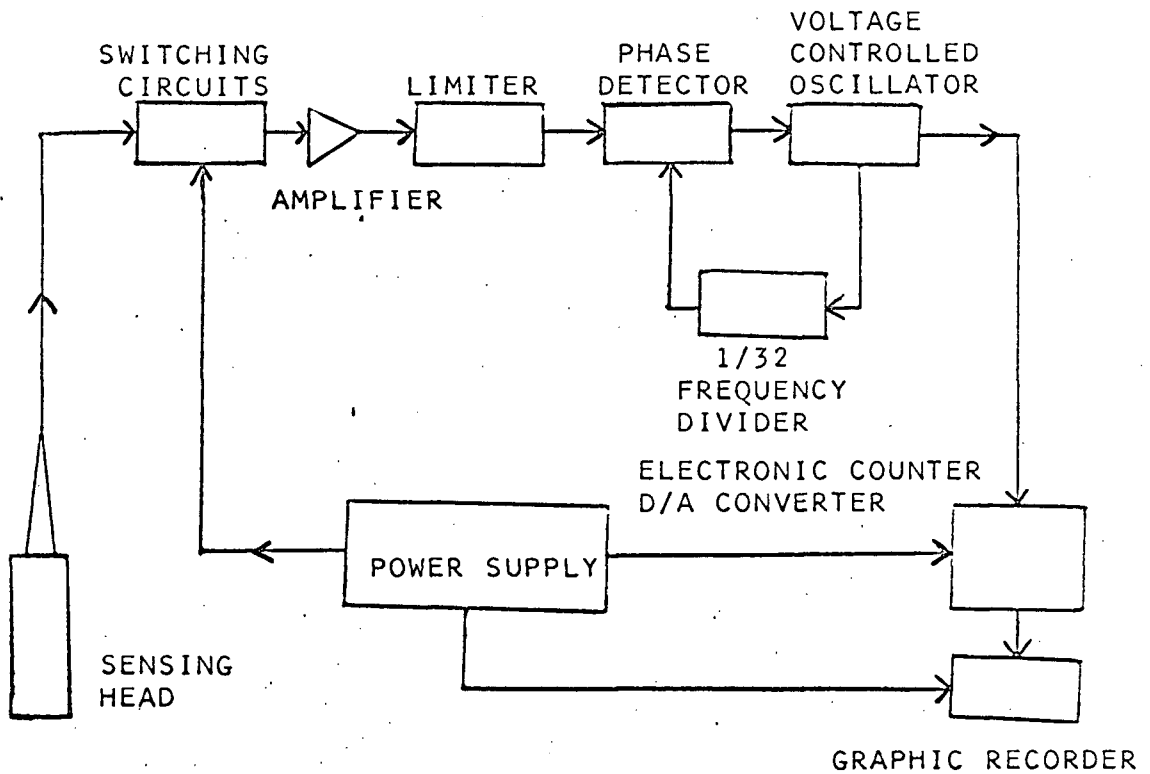
Figure 3   Schematic of the Varian-4937 Proton
            Precession Magnetometer

TABLE II

Specifications of Varian-4937
Proton Precession Magnetometer

Range	20,000-100,000 gammas
Accuracy	± 1 part in 10^5 (proton constant, 23.4875, is known to 8 ppm)
Sensitivity	± 1 gamma in all ranges
Sampling Rate	2, 6, 10, 60, 100, 300 seconds per count
Reference Frequency Stability	2 ppm per month

was towed about 600 feet behind the ship or over twice the length of the ship.

CHAPTER II

RUN TO THE SEAMOUNT

On May 28 the cruise began from Victoria, British Columbia. The final loading of the ship occurred in Vancouver. Then the Endeavor travelled north between Vancouver Island and the mainland. The voyage from the entrance into the Queen Charlotte Sound to the seamount is illustrated in Fig. 4. Navigation on the voyage was done by sunshots and dead reckoning. In the figure the circles show the places where the ship's positions were recorded from the bridge. We see that our destination, Bowie Seamount, is approximately at 53°18'N and 135°41'W. On this run magnetic and bathymetric measurements were made. A magnetic measurement was taken every 60 seconds; bathymetric measurements were made for all practical purposes continuously. Starting at 132°W, positions were recorded on an hourly basis. A plot of the magnetics and the topography versus distance from the main peak of the seamount is shown in Fig. 5. Having looked at the original records, one observed that there were several crests and troughs in the magnetic and the bathymetric records between the hourly positional readings. The positions of these crests and troughs were estimated. These extreme magnetic and bathymetric values are the circled ones in Fig. 5.

The region in which the cruise covered included

QUEEN CHARLOTTE
ISLANDS

BOWIE
SEAMOUNT

CONTINENTAL
CANADA

52°N

SHIP'S
COURSE

RAFF AND MASON
ANOMALIES

VANCOUVER
ISLAND
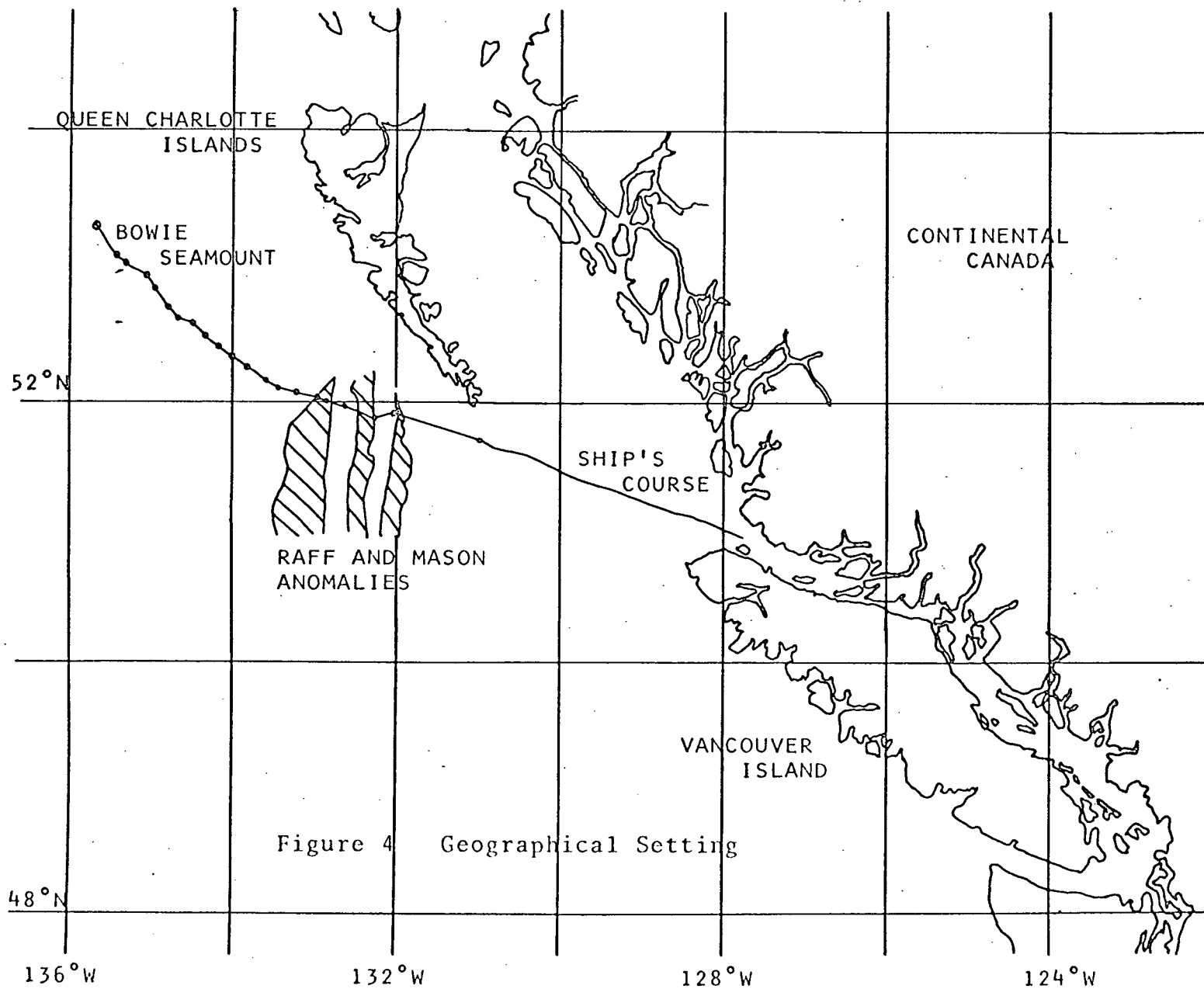
Figure 4   Geographical Setting

48°N

136°W   132°W   128°W   124°W
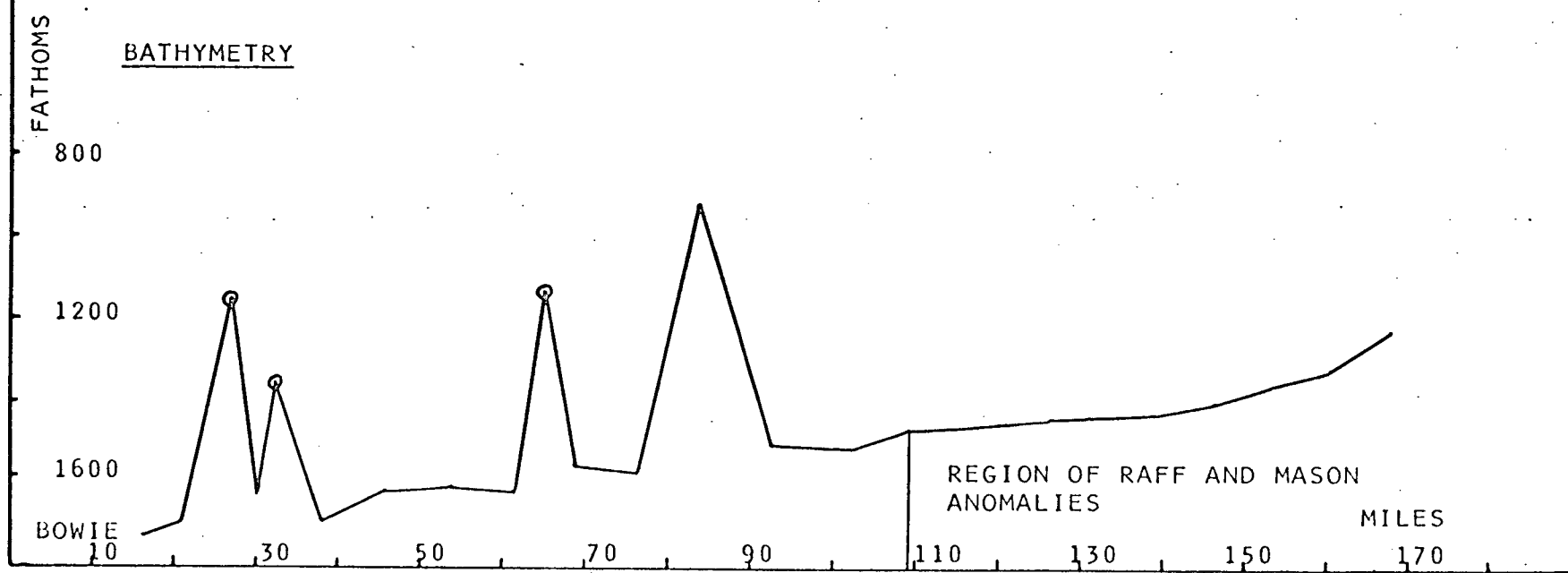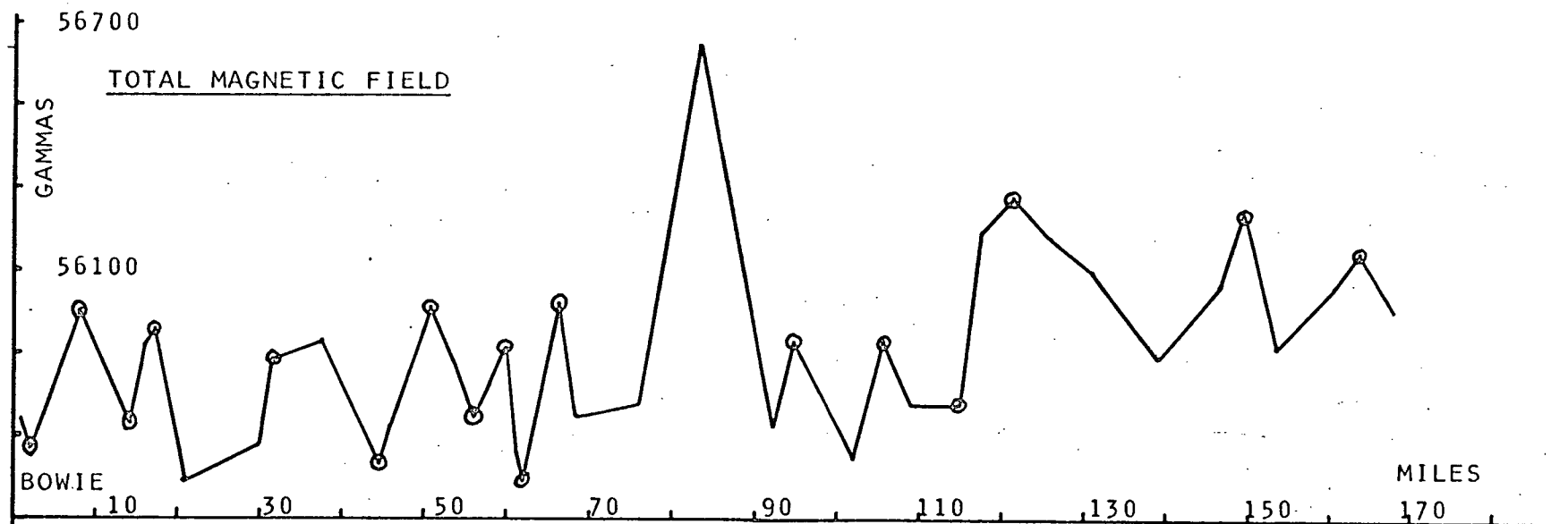
Figure 5   Magnetics and Bathymetry of the Run to Bowie Seamount

the magnetic lineations published by Raff and Mason (1961);
these are shown in Fig. 4 by letting the positive anomalies
be crosshatched. Fig. 5 illustrates the published Raff
and Mason lineations. As the ship proceeded from this
area to the seamount, the alternate positive and negative
lineations seem to continue. However, the situation is
complicated by the fact that the topography becomes irre-
gular. Thus it becomes difficult to tell whether the
observed cyclic highs and lows are due to topographical
features or to the continuation of the Raff and Mason
lineations. The importance of this becomes more than
academic when one determines a regional gradient. Note
that on approaching the seamount, one still has oscilla-
tions of the order of 200 to 300 gammas.

To go along with the geographical setting, Fig. 6
shows the topographical setting. This map is based on U.S.
Naval Oceanographic contour maps (1410N and 1411N) that
have recently become unclassified. In the region of inte-
rest, the navy had sounding lines every 5 to 10 miles.
The original maps were contoured every 100 fathoms. The
main observation to make is that Bowie Seamount has the
same lineations as do the other seamounts or for that
matter the same lineations of any of the shown contours,
i.e. lineations in a southwest to a northeast direction
and a corresponding one that is approximately perpendicular.

14

CONTOUR LINES IN FATHOMS
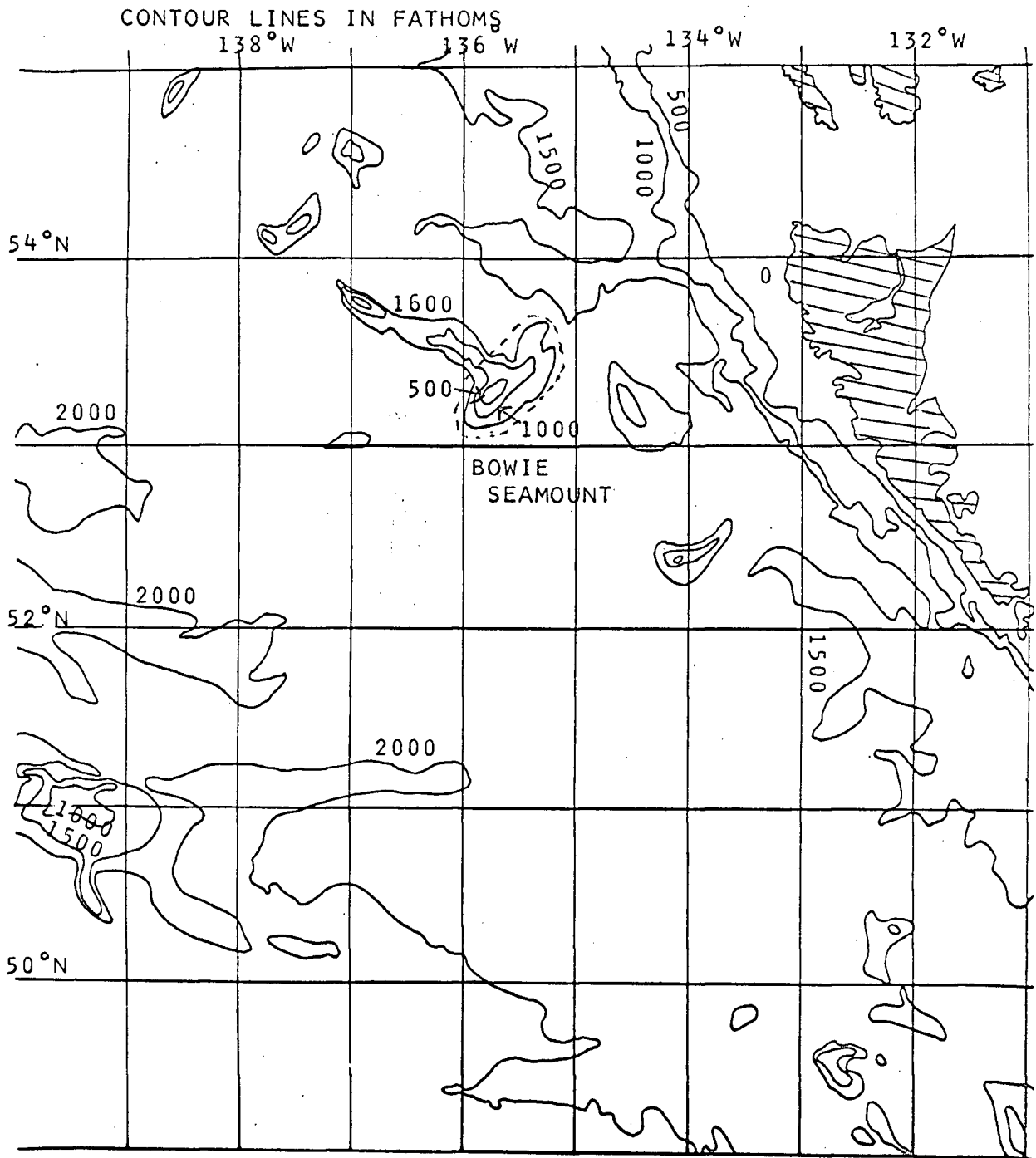
Figure 6   Topographical Setting

CHAPTER III

SHIP'S PATTERN

The Endeavor reached the seamount on May 31.
At 1400 P.S.T. the first attempt to anchor our buoy was
made; it failed. Due to a subsequent storm another attempt
was not made until the early hours of the 2nd of June.
The above illustrates some of the headaches of oceanographic
work. However, by 0430 P.S.T. all was ready for the taking
of magnetic and bathymetric measurements.

To get adequate coverage of the whole seamount
as quickly as possible - in case of equipment failure -
the ship first undertook the star pattern shown in Fig. 7.
Perhaps a more primary reason for the planning of the star
pattern was that there existed an uncertainty in how far
from the buoy the ship could be and yet pick up the buoy on
radar. Thus it was felt that if some dead reckoning had
to be done, radial paths to the buoy would give the most
accurately known tracks. However, the radar navigation
worked for the extent of the coverage. In order to get
cross-overs a type of spiralling square pattern was super-
imposed on the star pattern. Unfortunately, at all cross-
overs the two coincidental points are separated in time
by at least 24 hours. Thus it was impossible to correct
for daily magnetic variation from the data itself. Of
course with the very large gradients and with a position-
ing error of $\pm.2$ mile, one probably could not do so even

Figure 7

BOWIE SEAMOUNT

SHIP'S TRACK

CONTOUR INTERVAL - 100 fms

SCALE

NAUTICAL MILES

KILOMETRES
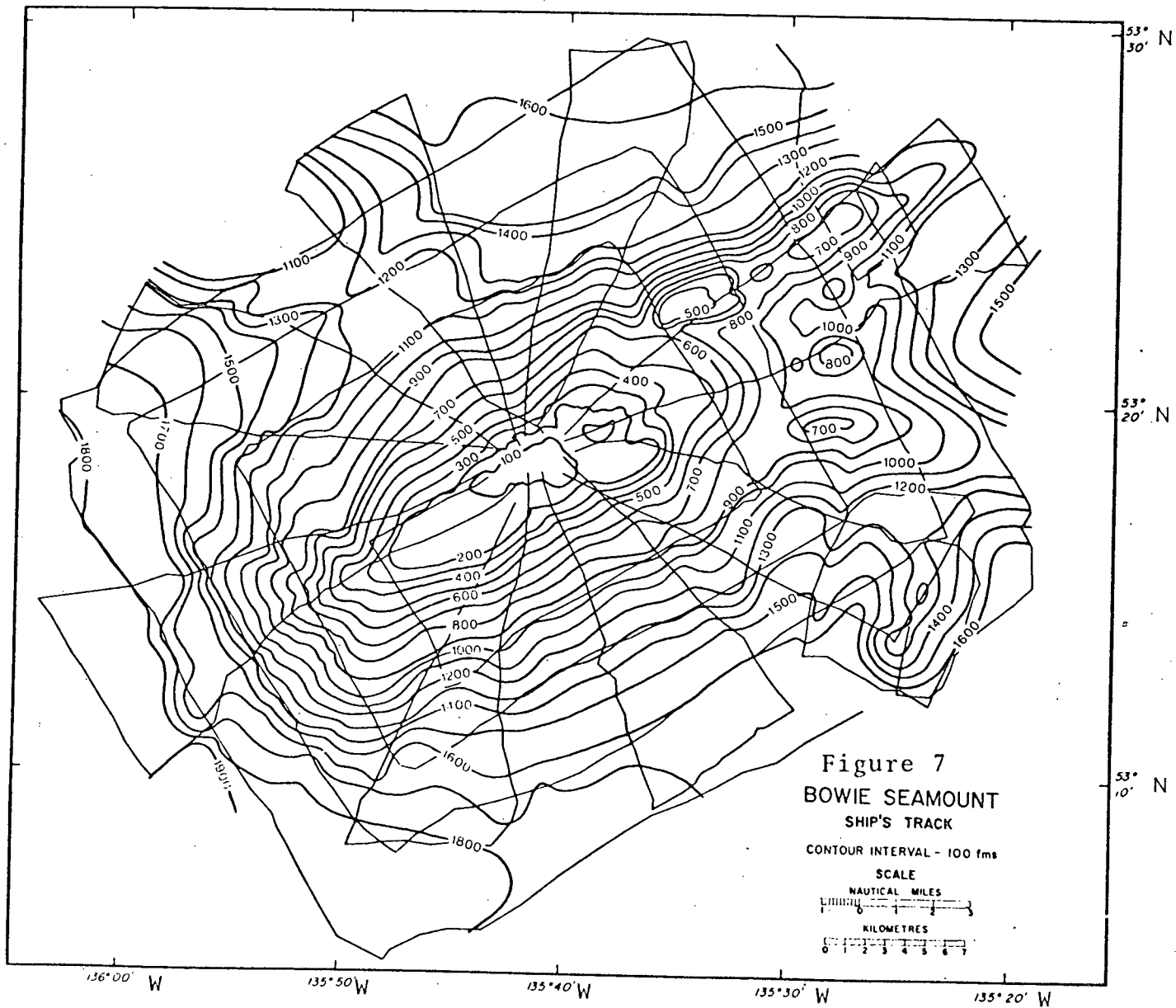
if the cross-overs were close in time. What was needed was a continuously recording magnetometer mounted on the buoy.

While making the star and the square patterns, the bathymetry was continuously recorded, but measurements of the total magnetic field were made at 20 second intervals. Position readings were usually taken at intervals of less than .5 of a mile.* In addition to the two principal patterns, a detailed pattern - Fig. 8 - was done around the buoy; however, only bathymetric measurements were made on this run.

The method of taking data was quite routine, a necessity for long periods of ship work. When one read a position aloud another recorded the range and azimuth. At the same time the magnetic and depth charts were marked. Then a data sheet was filled out giving the station number, time, range, azimuth, depth, and magnetic field. Altogether there were 741 stations in the star and square patterns and 160 in the small detailed run.

---

*A mile is being defined as 6,000 feet, for it was in such units that the navigational system measured the distance to the buoy.

Figure 8

BOWIE SEAMOUNT

SHIP'S TRACK OVER SUMMIT AREA

CONTOUR INTERVAL — 20 FATHOMS

SCALE

NAUTICAL MILES

KILOMETRES
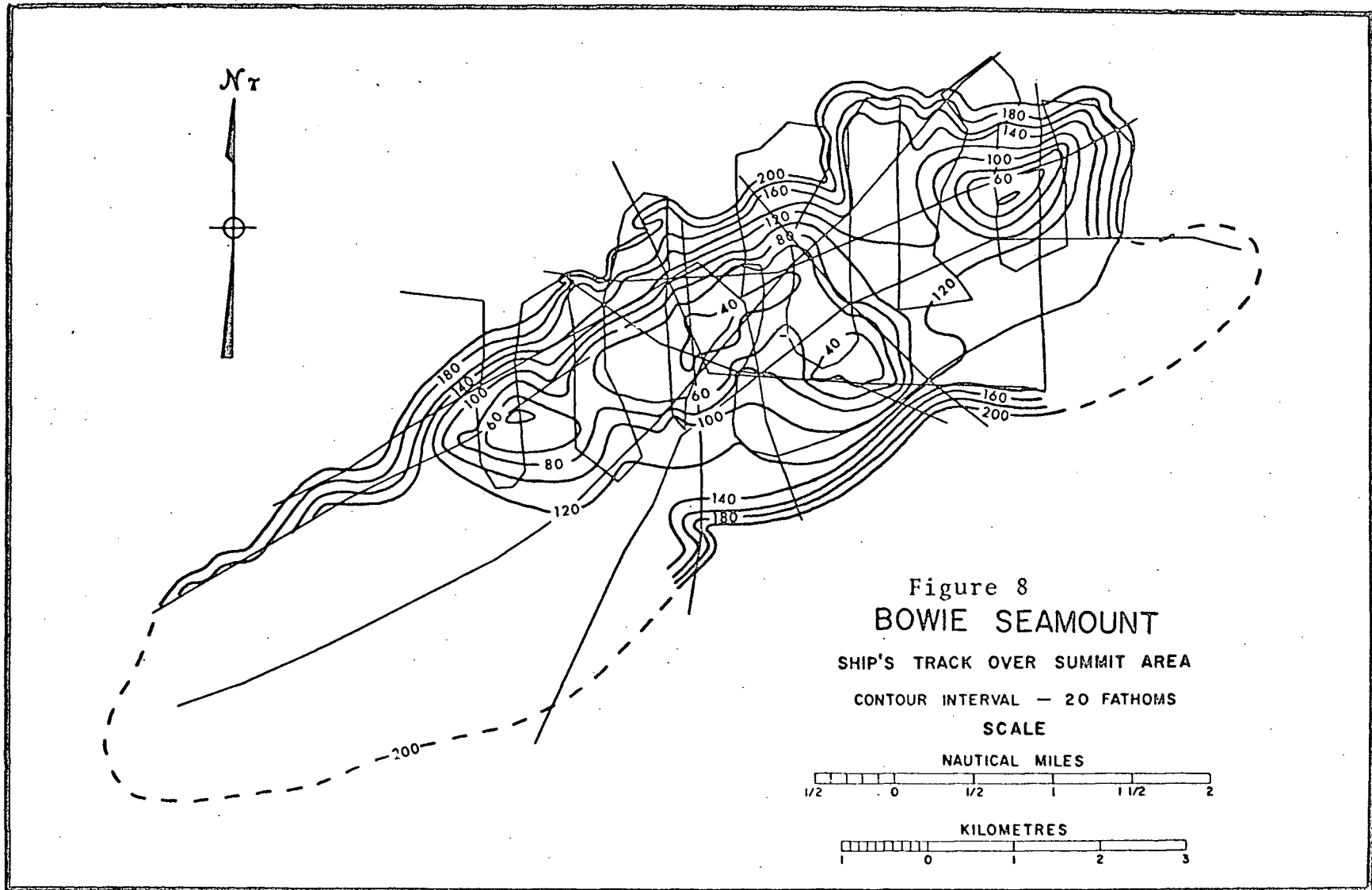
CHAPTER IV

BATHYMETRY

IV-1 Hand Contoured Maps

Looking at Figures 7 and 9, one sees the bathy-
metry of Bowie Seamount contoured at 100 fathom intervals*.
First, one notes that the ship's tracks just cover the
seamount. Second, one sees that the seamount is approxi-
mately elliptical around the center of the seamount. The
major axis is along a southwest to a northeast direction.
The southwest corner is closed but at the northeast end one
notes that the ellipse breaks into a ridge. In the transi-
tion to the ridge there seems to be several subsidiary
volcanic cones. In addition, one notes in the northwest
corner a ridge perpendicular to the semi-major axis.
By looking at Fig. 6 this ridge can be seen to lead to
another seamount called Hodgkin. As for the depth to
the abyssal plain, it appears to vary from 1600 to 1800
or 1900 fathoms as one travels from east to west.

Fig. 10 is a detailed bathymetry map of the top
of the seamount. The map is contoured in increasing in-
tervals of twenty fathoms starting from the 200th fathom
contour. One notes that there are four areas in which
there are 40 fathom contours. Thus one has a seamount
whose altitude is of the order of 10,000 feet or roughly

---

*Figures 7, 8, 9 and 10 were drawn by R. Herzer.

Figure 9
BOWIE SEAMOUNT
TOPOGRAPHY
CONTOUR INTERVAL - 100 fms
SCALE
NAUTICAL MILES
KILOMETRES

20
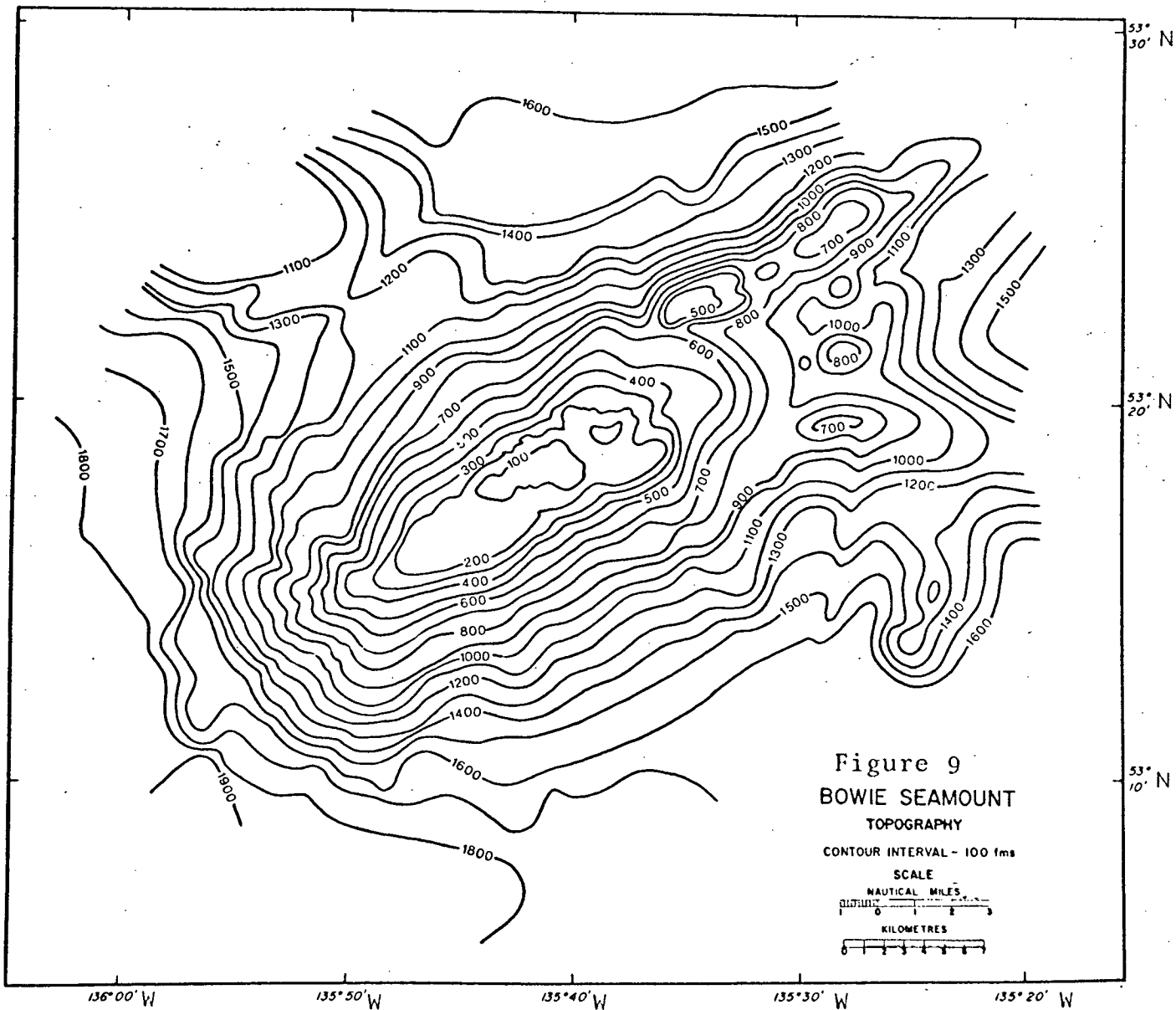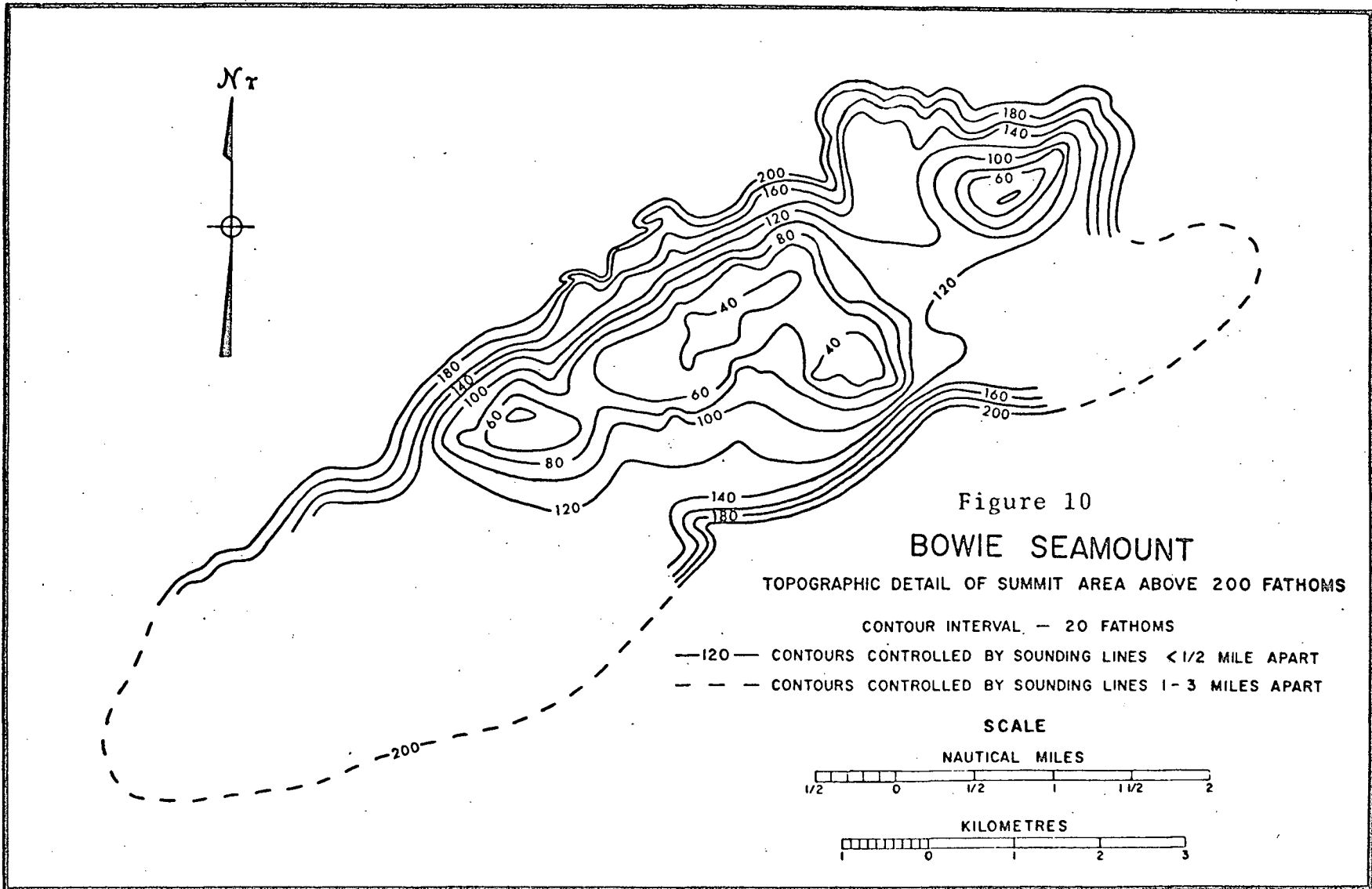
Figure 10

BOWIE SEAMOUNT

TOPOGRAPHIC DETAIL OF SUMMIT AREA ABOVE 200 FATHOMS

CONTOUR INTERVAL — 20 FATHOMS

—120— CONTOURS CONTROLLED BY SOUNDING LINES < 1/2 MILE APART

— — — CONTOURS CONTROLLED BY SOUNDING LINES 1-3 MILES APART

SCALE

NAUTICAL MILES
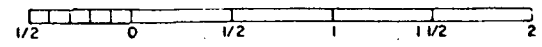
KILOMETRES
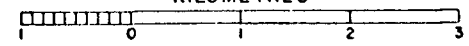
the size of Mt. Baker in the Northern Cascades of Washington.

Among the important features of Fig. 10 are the two substantial terraces that are located between the 40th and the 60th and between the 120th and the 140th fathom contours. The shallower terrace could be explained by wave action during the Pleistocene. It has been estimated that during the Pleistocene the level of the sea was lowered at times by more than 400 feet - Curry (1965). At present, there is no hint as to the age of the second terrace. However, due to the surfaces of sample rocks and to the underwater photographs both terraces appear to be wavecut. Another prominent feature in Fig. 10 is the very steep gradient in the southeast corner which could well be a relatively recent lava flow.

IV-2   Computer Contoured Map

To contour the total magnetic field measurements it was useful to use a computer program - Soup - written by W. J. Coultard (1968). The program takes the x, y, and z coordinates of the raw data to be contoured and generates values at the intersections of a square grid; x and y are the position coordinates of the field data and z is the height that corresponds to that position, i.e. magnetic field, depth below sea level, etc. To calculate the grid the program divides the region surrounding an intersection,

grid point, into octants and the nearest field point in
each octant is selected. However if there are no points
in any three adjacent octants, it is then arbitrarily
decided that there is insufficient data to calculate the
grid point and its value is set equal to -10^{30}. If there
are no such adjacent octants, the value of the grid point
becomes the weighted average of the selected points using
a weighting function of $1/d^2$, where d is the distance
from the nearest octal point to the grid point. The number
of grid lines in the x-direction is chosen by the user.
Along with this number the maximum and the minimum values
of x. determine the size of each square. The number of
grid lines in the y-direction is determined by the maximum
and the minimum values of y and by the size of the square.
On calculating the intersections, the program then yields
a contour and a perspective plot of the calculated grid.
For the perspective plot, the maximum value of the z
component is arbitrarily set equal to .3 of the distance
between the maximum and the minimum values of x . Unless
otherwise specified the perspectives are drawn looking
down at an angle of 45 degrees and rotated about 20 degrees.

Fig. 11, a computer contour plot of the bathymetry
of Bowie Seamount, illustrates the use of this program.
Looking back at Fig. 9, one notes that, despite the fact
that the contour interval of the computer plot is twice
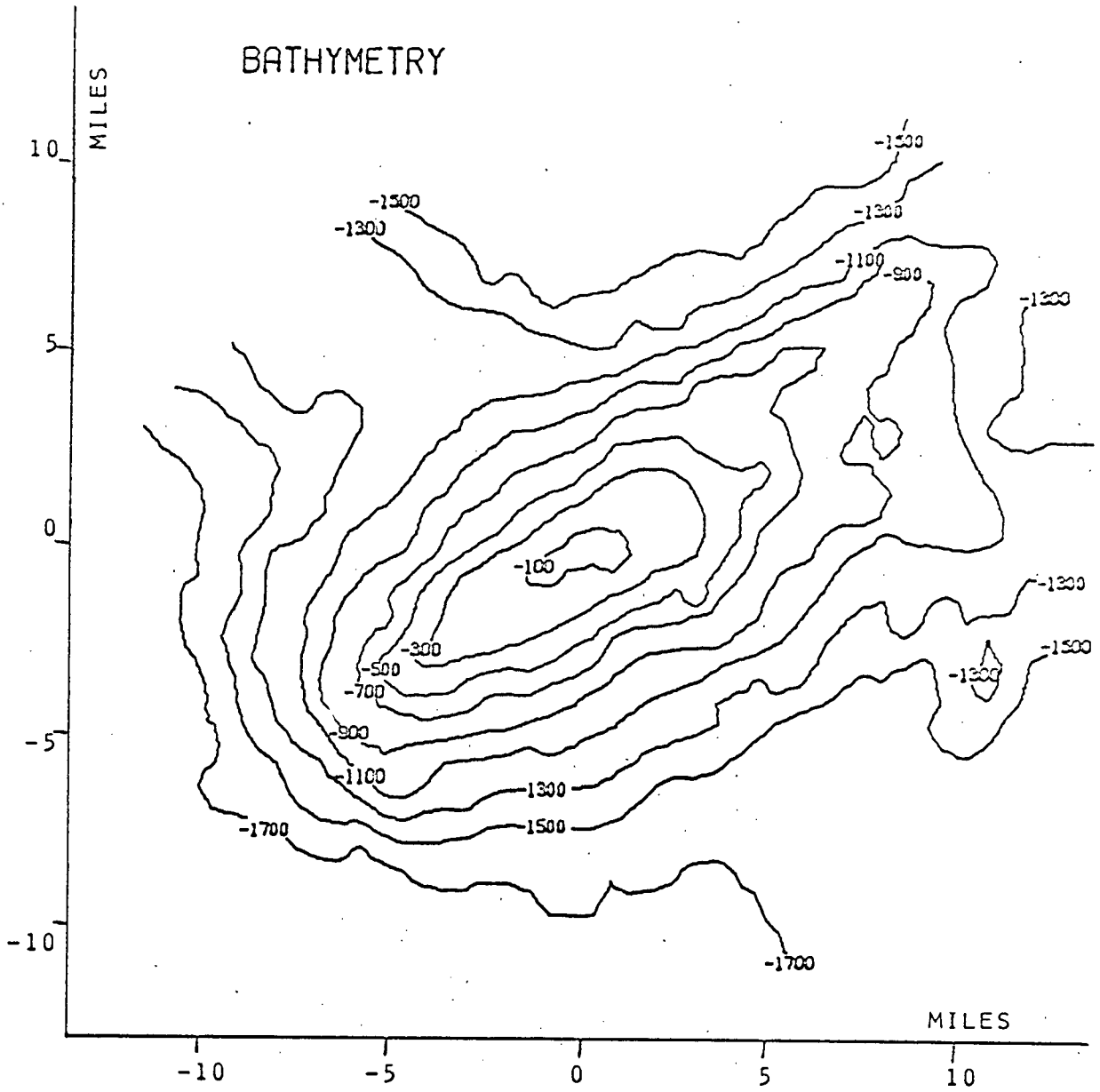
Figure 11   Computer Contoured Bathymetry

the value of the hand contoured plot, there is good agreement between Figures 9 and 11. Though some people may still prefer to use the hand contoured plot for bathymetry, it would seem quite adequate to use the computer's version for geophysical data. For interest, the perspective plot of the bathymetry is reproduced in Fig. 12.

Figure 12   Perspective of
BATHYMETRY

N

30 MILES

30 MILES

E
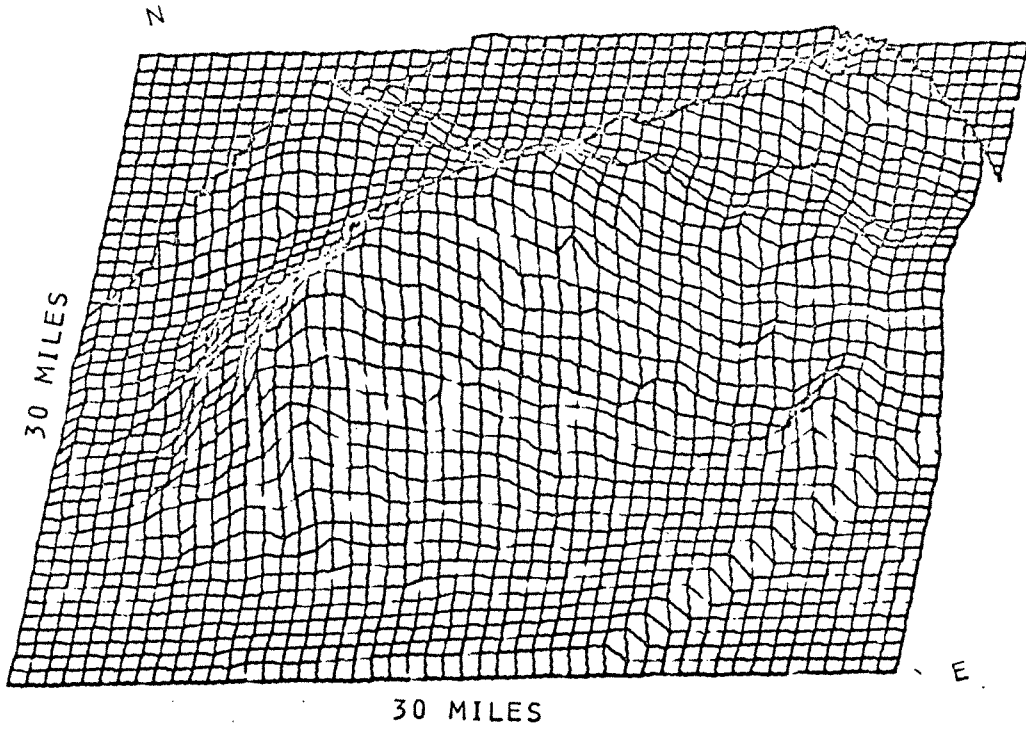
CHAPTER V

PHOTOGRAPHS AND ROCK SAMPLES

V-1 General Comments

Looking at Fig. 13*, one notes that there were 4 underwater camera stations. Altogether there were about 500 well developed photographs. The success of the photography was due to the fact that a pinger was attached to the camera setup. A pinger is merely a device which sends accoustical signals in all directions. Hovering over the setup, the ship picks up the signals directed straight up and the ones reflected straight up from the ocean floor. The time delay between the two signals yields the height of the pinger and thus the camera setup above the topography.

Rock samples were only taken by means of a dredge and a grab bucket, though a core was unsuccessfully attempted. On the 1968 cruise there were 3 dredge and 2 grab stations; while on the 1967 cruise there were 6 dredge and 7 grab stations. The distribution of the sampling stations can be seen in Fig. 13.

A detailed analyses of the photographs and the rock samples will be presented by Herzer (1969). The general characteristics of the rock samples are their basaltic

―――――――――――――――――――――――――――――

*Fig. 13 was drawn by R. Herzer.

DETAIL OF SAMPLE LOCATIONS ON SUMMIT

NAUTICAL MILES

CONTOUR INTERVAL – 20 fms.

LEGEND

DREDGE

GRAB

CAMERA

CORE

Figure 13
BOWIE SEAMOUNT
SAMPLE LOCATIONS
CONTOUR INTERVAL – 100 fms
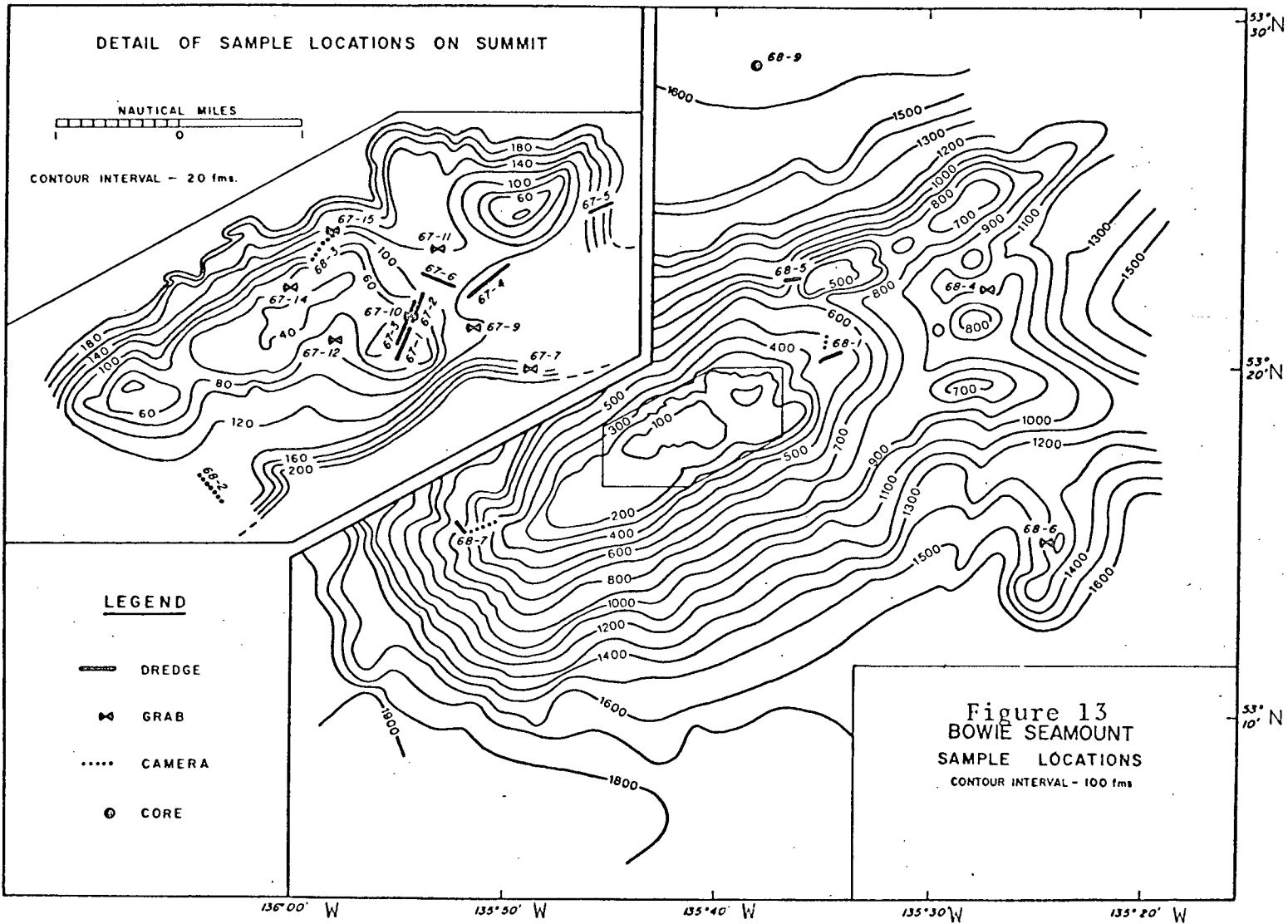
composition and their volcanic origin. The volcanic origin is indicated by flows in the photographs and by the macroscopic textures of the rock samples. Of a more specific nature, one finds that the rocks - fine grained, even glassy - become more vesicular as one approaches the summit of the seamount. This is to be expected as the hydrostatic pressure lessens with lessening depth, allowing the escape of gases and thus leaving small cavities in the lava. An exception to this is a rock picked up at station 67-7. This rock, located at the southeast side of the 150 fathom contour, is crystalline and nonvesicular leading to the possibility that this rock appeared on the surface after erosion occurred, i.e. the eruption took place underwater and this rock was subsequently exposed by erosion. This is inferred because in this way the sample would not have been quickly cooled, thus allowing crystals to form and the slow escape of gases leaving it nonvesicular. In fact one might surmise that it is part of a dyke or perhaps even a volcanic vent.

V-2   Remanence and Susceptibility

   V-2-1   Rock Magnetism

      In the presence of a magnetic field, i.e. the earth's magnetic field, a rock becomes magnetized by induction. The strength of the induced magnetization of the rock depends on the susceptibility of that rock. When the external field is removed most of the magnetization

disappears. Besides the induced magnetization of the rock, there is its remanent magnetization designated by NRM, natural remanent magnetism. NRM is often called fossil magnetism, for it was acquired in its past. There are three primary ways of achieving NRM. First, TRM, thermoremanent magnetism, is obtained by cooling rock material from its Curie Point in the presence of a magnetic field, i.e. the earth's magnetic field. TRM is the primary source of NRM in igneous rocks. Second, CRM, chemical remanent magnetism, is obtained by chemical processes, again in the presence of the earth's magnetic field. Finally, DRM, depositional remanent magnetism, occurs in sedimentary rocks by the orientation of small grains of magnetic material. For all three cases, the direction of NRM is dependent on the direction of the earth's field at the time of the magnetization of the rock. If the earth's magnetic poles were reversed at the time of the rock's magnetization, the rock's NRM will be in the opposite direction to the rock's induced magnetization. Theoretical methods have been published on how a rock could have a reversal in its magnetization independent of changes in the earth's main magnetic field. However these self-reversals are rare in nature - Irving (1965).

V-2-2 Magnetic Properties of Samples

. Among the many rock samples obtained from Bowie
Seamount a few were large enough and sturdy enough so that
cores could be taken. Thus 7 samples were sent to Ottawa
to the Division of Geomagnetism of the Department of Energy,
Mines, and Resources. The susceptibilities of three of
the samples and the NRM of all 7 were made by E. Irving
of that group and by John Steele of the Geophysics Depart-
ment of the University of British Columbia. Unfortunately,
the orientations of the samples were not known; thus the
direction of the remanent magnetism could not be indicated.
The results of these measurements are made in Table III.
Besides taking the normal average and standard deviation,
the logs of the measured values were taken, averaged, and
then the antilog was found. This was done in compliance
with a paper by Irving (1966) in which he felt that such
a statistic should be given in all future work stating
susceptibilities and remanences. This feeling arose from
the fact that Irving found that for the Torridonian Sand-
stones histograms of the number of samples versus the
$\log_{10}$ of the intensity of magnetization shows a good fit
to the logarithmic normal function. In calculating these
statistics, the value of the sample from Hodgkin Seamount
has been deleted. The results are in Table IV. Consider-
ing the changes in order of magnitude of remanence in
differing basalts, the two types of mean for the remanence

TABLE III

Magnetic Samples

Sample Station	Year	General Description	Susceptibility* (c.g.s.)	Remanence** (c.g.s.)
7	1967	Diabasic basalt dyke rock, Approx. 150 fathoms, Southside	$1,414 \times 10^{-6}$	7.74×10^{-3}
14	1967	Vesicular block, Central peak near 45 fathom terrace, Northside		1.63×10^{-3}
1	1968	Finely vesicular basalt block, Approx. 500 fathoms, Northeast flank	$1,263 \times 10^{-6}$	12.15×10^{-3}
1	1968	Vesicular flow, Approx. 500 fathoms, Northeast Flank		5.0×10^{-3}
8	1968	Vesicular basalt block, Hodgkins Seamount, Approx. 450 fathoms	95.3×10^{-6}	$.62 \times 10^{-3}$
14	1968	Location same as 67-14 (at buoy)		6.98×10^{-3}
7	1968	Pillow fragments, Southwest side seamount, Approx. 800 fathoms		11.0×10^{-3}

*error in susceptibility measurements $\pm 5\%$
**error in remanence measurements $\pm 5\%$

TABLE IV

Averages of Samples (CGS Units)

	mean	standard deviation	antilog of mean log.
Susceptibility	1339×10^{-6}	106.8×10^{-6}	1336×10^{-6}
Remanence	8100×10^{-6}	14.4×10^{-3}	6860×10^{-6}

are quite similar. According to Irving, "It is perfectly clear that whatever anomaly there is over Bowie Seamount is due to the remanence".

CHAPTER VI

ORIGINAL MAGNETIC DATA

VI-1 Data Recording

When the magnetic survey was in operation,
there were 741 position stations. At the time of these
stations, the analog recorder was given a hand time mark.
There was also a digital recorder which similarly recorded
measurements at twenty second intervals. However, the
oscillator controlling the instrument's clock was inac-
curate, giving 61 seconds to the minute. Actually, the
crude test done on cruise indicated that it was slightly
variable; however, the tests were not accurate enough
to give an estimate other than 61 seconds to a minute.
At erratic intervals the personnel would correct the
instrument's clock to the ship's time but without record-
ing their deed. Further, in order to get magnetic read-
ings synchronous to bathymetric ones, hand time marks
were put on the analog and the digital outputs and on the
depth recordings at each time a position was recorded.
For some reason the time marks were more shoddily put
on the digital output than on the analog, introducing a
larger error in the digital output as to which recorded
value actually corresponded to a time mark. Consequently,
it was decided to use the analog recording in analyzing
the magnetic data. Though the manufacturer claims an
accuracy of one gamma on the digital and its corresponding

visual output, the analog seemed to agree with the visual output to 3 gammas.

The analog data was hand digitized, and then the station number, time, range, azimuth, depth, and the magnetic field was punched on computer cards. For the sake of convenience the cards were repunched converting the originally recorded hours and minutes to hours and using x, y coordinates where the origin is at the buoy and where the positive x and y axii are respectively pointing to the geographical East and North. Along with the original analog and digital output, a permanent deck of the above is to be placed at the disposal of the Department of Geophysics of the University of British Columbia.

VI-2 Diurnal Corrections

Due to atmospheric effects, the magnetic field at a given spot will vary. If possible this variation should be removed from the observed data. Ideally, one would want the total field being recorded by a magnetometer at some fixed point in the region of interest, i.e. on top of the buoy. This would not only remove the daily or diurnal variation but also the local magnetic variation. However, there was no such recording and to remove the magnetic variation, magnetograms from May 27th to

June 5th were obtained from stations of the Dominion
Observatory at Victoria, British Columbia and Meanook,
Alberta. From Table V one can calculate that the dis-
tance from Bowie Seamount to Victoria is about 720 miles
and to Meanook is about 880 miles. With such distances
one could not directly use the magnetograms from these
stations to correct for local magnetic variations. Thus
it was decided to take the records from two or three of
the quietest days in this period, average their readings,
and then use the averages to correct for daily variation.
The daily variation is global and is primarily dependent
on geomagnetic latitude. In calculating the diurnal,
the records were hand digitized at half hour intervals.

To correct for the diurnal two time corrections
were needed to be made on the averaged variations. First
was the trivial correction of converting the universal
time to the ship's time. Second was the correction re-
sulting from the daily variation at a constant geomagnetic
latitude travelling westward with time, due to the fact
that the daily variation is primarily solar in origin and
that the earth rotates. Then a program was written which
subtracted from the original data the total diurnal varia-
tion using the time corrected data from Meanook, from
Victoria, and from combining the data from Meanook and
Victoria by means of a linear interpolation with respect

TABLE V

Magnetic Stations

Station	Geographical Latitude	Geographical Longitude	Geomagnetic Latitude	Geomagnetic Longitude
Bowie Seamount	53.30°N	135.68°W	56.4°N	276.8°E
Victoria	48.52°N	123.41°W	54.3°N	292.7°E
Meanook	54.62°N	113.33°W	61.8°N	301.0°E

to geomagnetic latitude. Then with the approximately 60 cross-over points in the ship's pattern, the program calculated the discrepancy in the magnetic measurements by taking the value due to the star pattern minus the value due to the spiralling square. The program then found the square root of the average square of the dis-crepancy. This was done for the original data and for the original data corrected with the data from Victoria, from Meanook, and from the linear interpolation between the two; respectively, the results were 45.3, 44.5, 42.0, and 43.5 gammas. A surprise is that the data corrected from Meanook gave the smallest value but Victoria is much closer to Bowie Seamount in geomagnetic latitude than Meanook. However, the results are not significant and the original data was used for the analysis of the total magnetic field measurements.

VI-3 Contour of the Original Data

Entering the original data into the contouring program mentioned in Chapter IV, one gets the contour map shown in Fig. 14 and the perspective in Fig. 15. Similar to the topography, there is a strong SW to NE lineation and there is also a less distinct trend from the buoy towards the NW. There is a relative high around the origin and it extends to an extensive region in the East; however, there is a deep low to the immediate SW of this

Figure 14
# TOTAL MAGNETIC FIELD OF BOWIE SEAMOUNT
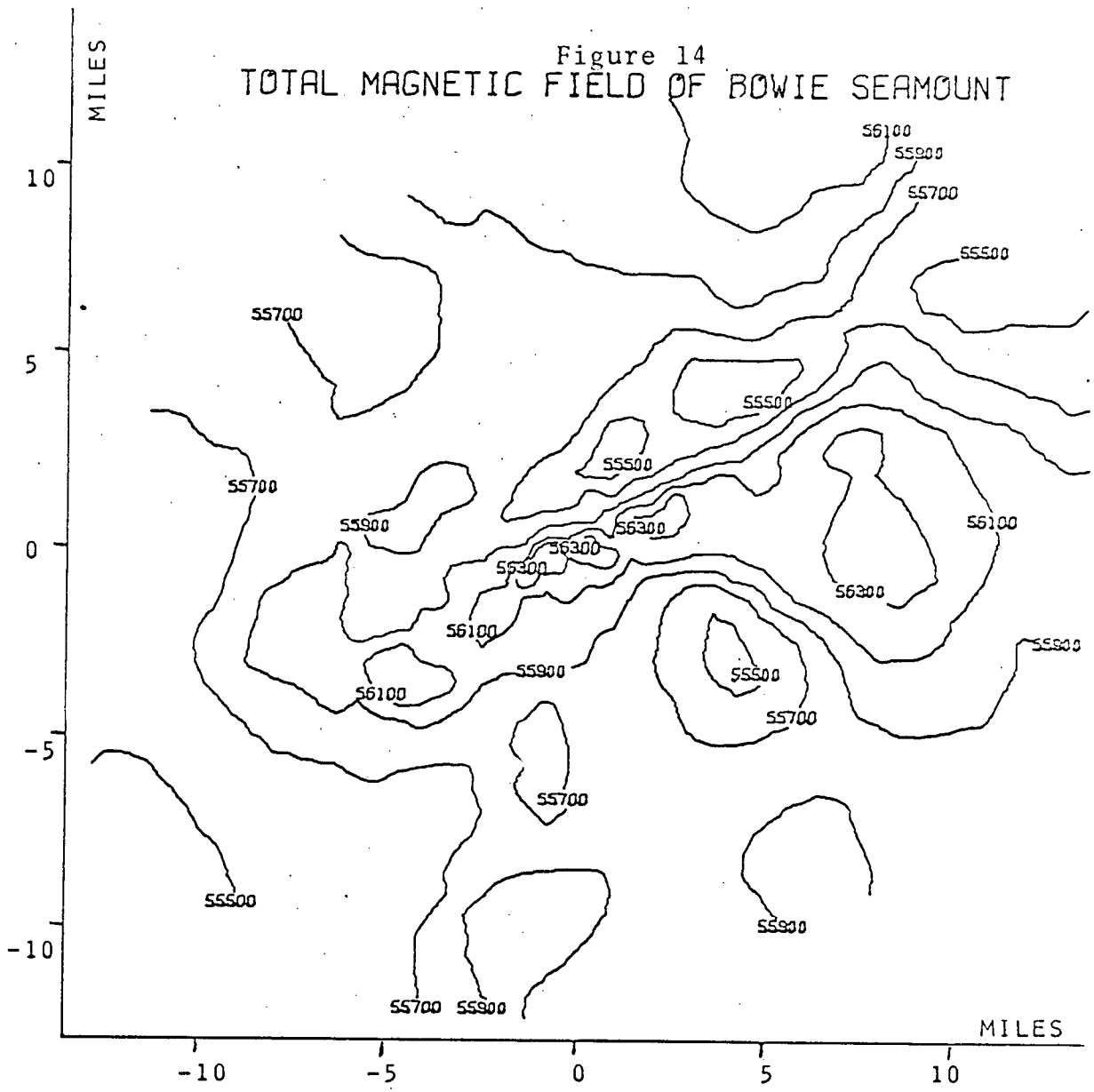
Figure 15   Perspective of
TOTAL MAGNETIC FIELD OF BOWIE SEAMOUNT
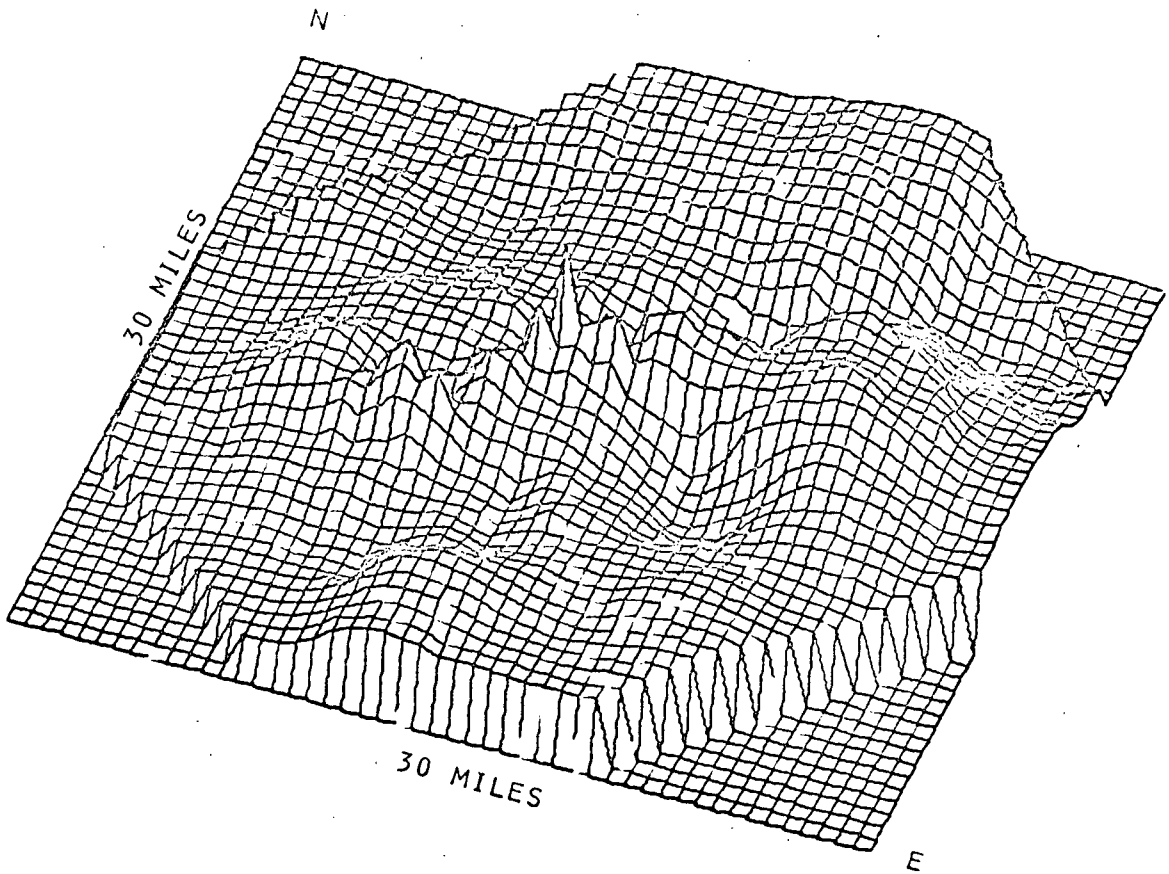
high.   On the whole the total magnetic field plot does
not show as much symmetry as the topography.

CHAPTER VII

OBSERVED ANOMALY

Except for the run to the seamount, the magnetic field measurements did not really extend beyond the topographical limits of the seamount. Therefore the regional magnetic field, i.e. the total observed field minus the effects of the seamount, could not realistically be determined by the data obtained on the cruise. To determine the regional, data was taken from an air-borne survey done by the Dominion Observatory in 1958. The plane's tracks are shown in Fig. 16, where the area covered by the data used to determine the regional is marked off by x's and the actual data is given in Table VI. To calculate the regional a method of least squares was applied to the data. In doing so the regional was assumed to take the form of a plane, i.e. $z = ax + by + c$ where x and y are expressed in miles and are respectively positive in an east and north direction from the buoy and where z is in gammas. Converting the positions of the data into x_i , y_i coordinates with respect to the buoy, setting $f(a,b,c)$ equal to $(ax_i + by_i + c - z_i)^2$, taking the three partial derivatives of $f(a,b,c)$, equating the derivatives to zero, and finally solving the resulting equations for a , b , and c ; one gets $z = ((3.8x + 6.2y)/\text{miles} + 56105)$ gammas . Upon substitution of $a=3.8$, $b=6.2$, and $c=56105$ into the following

43

Figure 16
AIRBORNE MAGNETIC SURVEY
1958
CANADA
SCALE

BOWIE

Map. №7
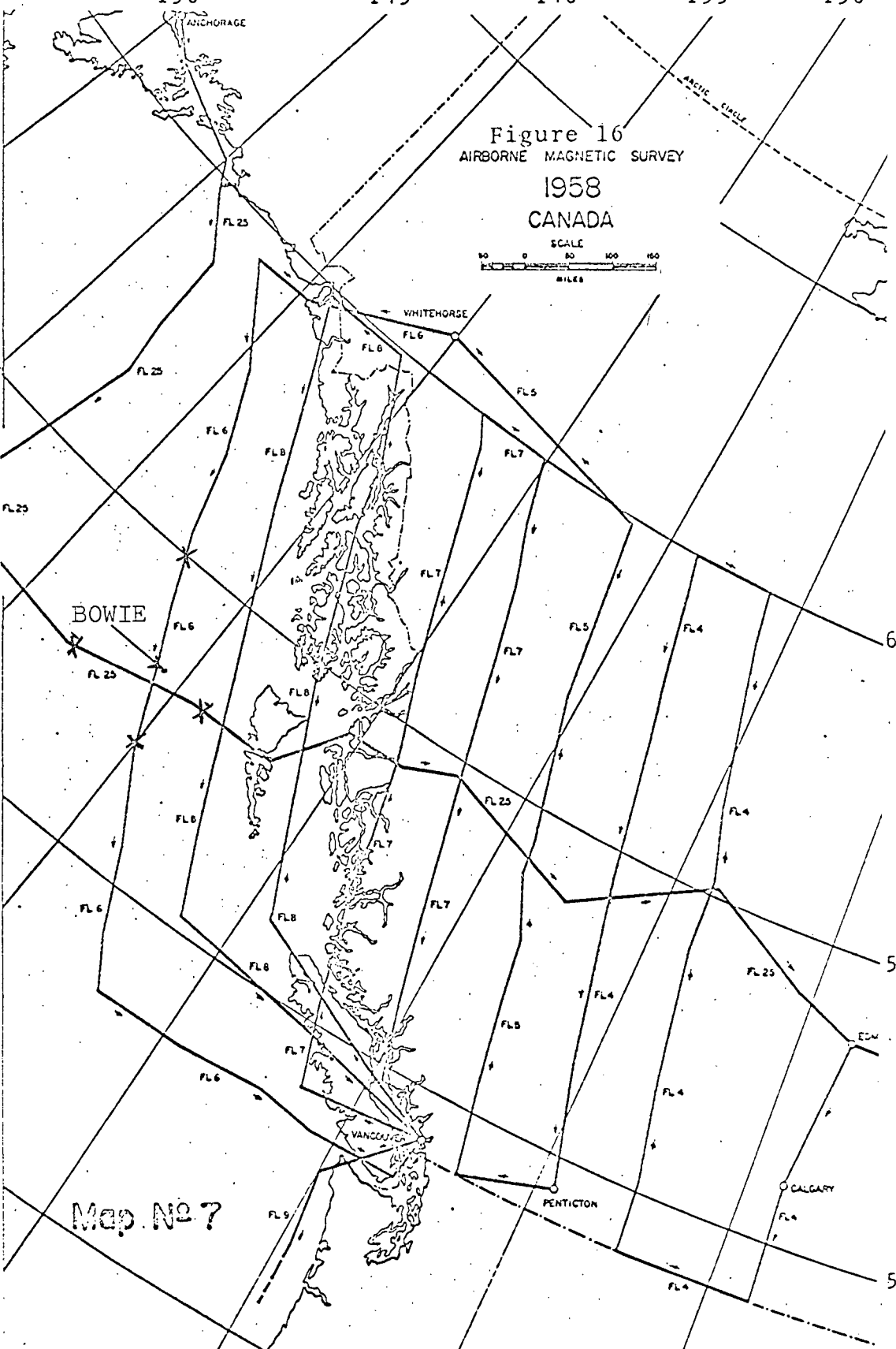
TABLE VI

Regional Data

Flight	Station (i)	Latitude	Longitude	Total Magnetic Field (gammas)	Magnetic Declination	Magnetic Inclination
25	1	52°37'N	137°52'W	55440		70°34'N
	2	52°40'N	137°37'W	55620		70°40'N
	3	52°43'N	137°19'W	55690		70°59'N
	4	52°46'N	136°52'W	55770		71°12'N
	5	52°51'N	136°20'W	55860		71°21'N
	6	53°07'N	135°10'W	56060		71°26'N
	7	53°10'N	134°33'W	56230		71°22'N
	8	53°11'N	134°04'W	56230		71°31'N
6	9	55°00'N	137°16'W	56520	27°24'E	72°34'N
	10	54°48'N	137°08'W	56480	27°12'E	72°42'N
	11	54°36'N	136°58'W	56370	27°04'E	72°40'N
	12	54°25'N	136°48'W	56320	27°00'E	72°33'N
	13	54°13'N	136°39'W	56240	26°54'E	72°20'N
	14	54°01'N	136°29'W	56260	27°18'E	72°12'N
	15	53°50'N	136°20'W	56300	26°36'E	72°08'N
	16	53°38'N	136°10'W	56120	26°18'E	72°05'N
	17	53°27'N	136°02'W	56010	26°36'E	71°59'N
	18	53°16'N	135°53'W	56090	26°30'E	71°36'N
	19	53°05'N	135°46'W	55990	26°30'E	71°26'N
	20	52°53'N	135°37'W	55890	26°24'E	71°23'N
	21	52°42'N	135°30'W	55830	26°18'E	71°27'N
	22	52°32'N	135°22'W	55870	26°06'E	71°12'N
	23	52°20'N	135°13'W	55850	26°00'E	71°06'N
	24	52°09'N	135°05'W	55730	25°42'E	70°59'N

44

expression:

$$\sum_{i=1}^{24} \frac{((ax_i + by_i + c - z_i)^2)^{\frac{1}{2}}}{24} \quad ,$$

the average residual is found to be 42.36 gammas. The next step was to subtract the regional from the observed magnetic values, yielding an observed anomaly. In the substraction the original field points were used and not grid points derived from the earlier contour map. The contour of the observed anomaly is in Fig. 17. The main observation is that the magnetic field pattern has not been drastically changed from that in Fig. 14. However, one should note that Bowie Seamount has a basically negative anomaly. This implies that at least most of Bowie Seamount is reversely magnetized.

Figure 17

OBSERVED TOTAL ANOMALLY OF BOWIE SEAMOUNT
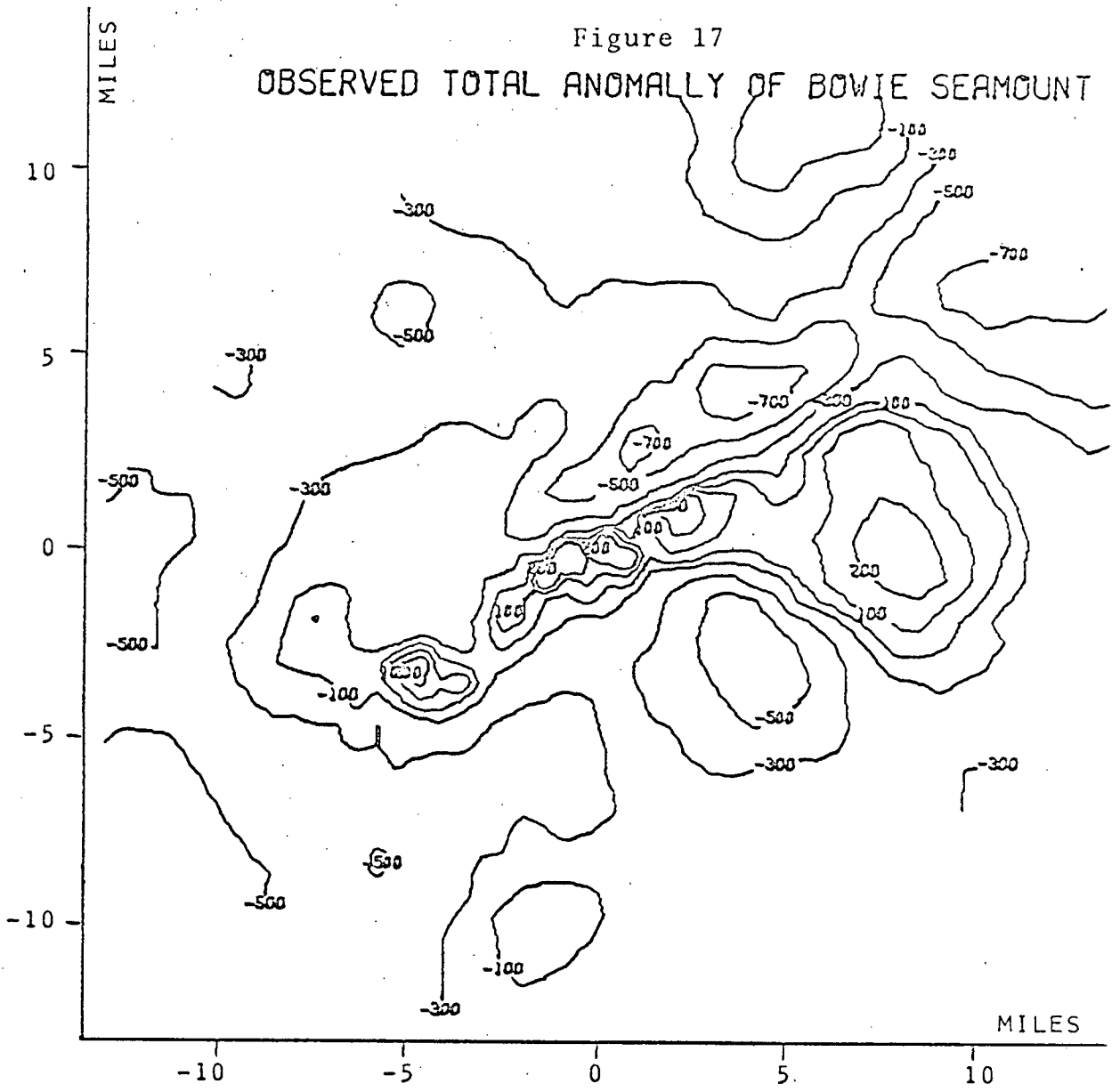
CHAPTER VIII

THREE DIMENSIONAL ANALYSIS

VIII-1 <u>Nature of Terrain Correction</u>

With the regional and thus the observed anomaly
determined, one is ready to subtract the effect due to
the terrain itself. Obviously, if one has chosen the
regional correctly and one makes an exact correction due
to the seamount, then the residual anomaly will be zero.
There are several reasons why this will not happen.
First, an approximation must be made of the seamount's
shape. Second, if one does not assume a uniform intensity
of magnetization or at least uniform in discrete portions
of the seamount, then the calculations will be very dif-
ficult. Third, one probably does not know the suscepti-
bility and/or remanence of the terrain any better than a
factor two, much less its spatial distribution. In addi-
tion, if from a tremendous amount of samples one knew the
surface distribution well, one still would not know how
the magnetic properties varied with depth and one would
not have information as to whether the terrain was com-
posed of rocks some of which were reversely magnetized
while others were normally magnetized. However, one would
hope to make some guesses about some of these unknowns
on the basis of a few simple models. For this study the
simple models were made using a three dimensional analysis

program written by Talwani (1965).

VIII-2   Theory and Method of Talwani's Program

The following has been abstracted from "Computation with the Help of a Digital Computer of Magnetic Anomalies Caused by Bodies of Arbitrary Shape" by Talwani (1965).

Let us look at Q , a topographical feature, in Fig. 18. For the volume element $\Delta x \Delta y \Delta z$ the scalar magnetic potential - $\vec{B} = -\vec{\nabla}V$ - is given in cgs units by*

$$(1) \qquad V = \frac{\vec{u} \cdot \vec{R}}{R^3}$$

where $\vec{u}$ is the magnetic moment of the volume element and $\vec{R}$ is the indicated distance vector. Let $\vec{J}$, the intensity of magnetization of Q , be uniform, making $\vec{u}$ equal to $\vec{J}\Delta x \Delta y \Delta z$ and thus yielding V to be given by

$$(2) \qquad V = \frac{J_x \cdot x + J_y \cdot y + J_z \cdot z}{R^3} \ \Delta x \Delta y \Delta z$$

where J_x , J_y , and J_z are the components of $\vec{J}$. What one could call the components of the magnetic field anomaly due to Q is

$$\Delta X = -\iiint \frac{\partial V}{\partial x} \ dx dy dz$$

---

*Reitz, J. and Frederick J. Milford, Foundation of Electromagnetic Theory, 1962.
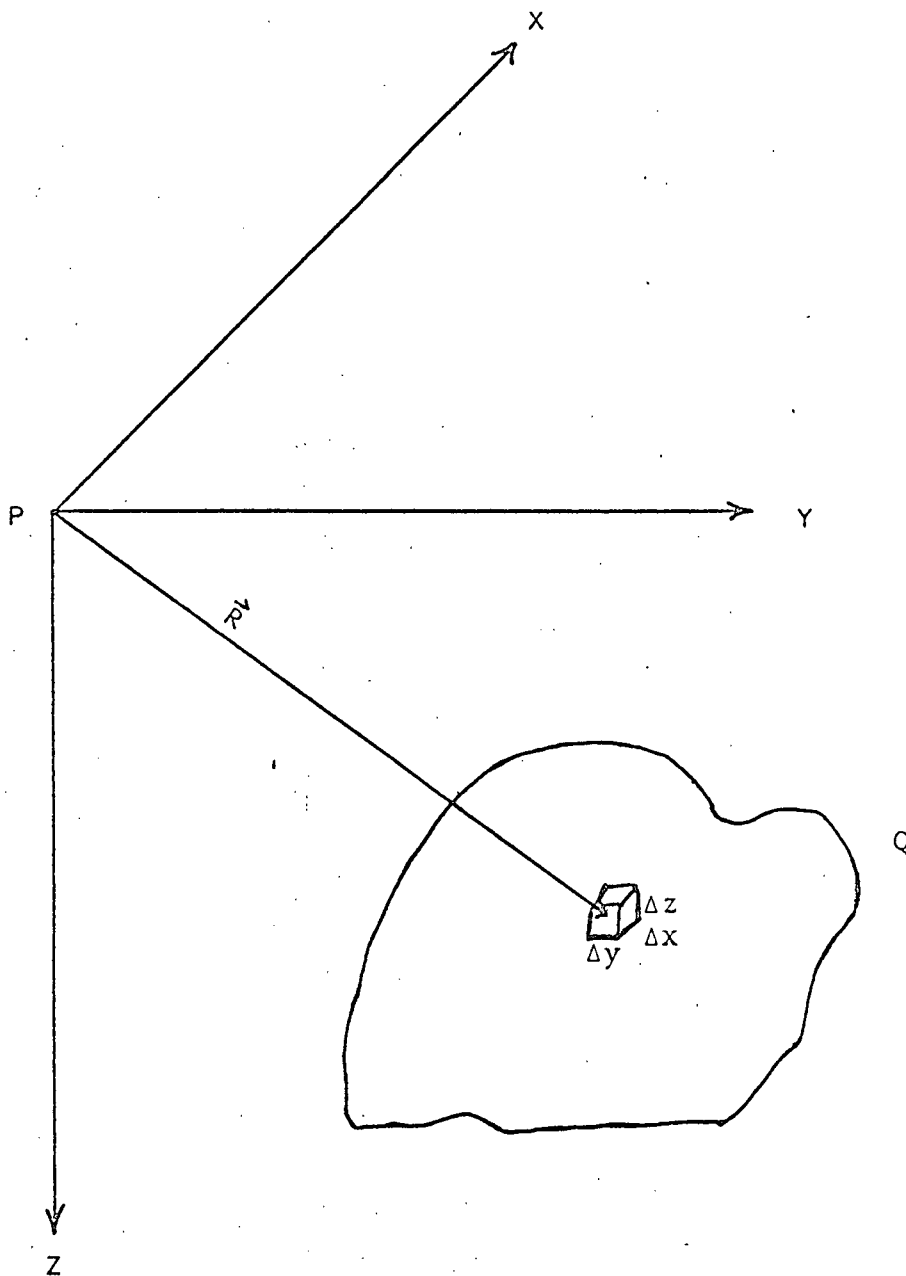
Figure 18   Coordinate System and Topographical
            Feature   Q   .

$$\Delta Y = -\iiint \frac{\partial V}{\partial y} \; dxdydz$$

$$(3) \quad \Delta Z = -\iiint \frac{\partial V}{\partial z} \; dxdydz$$

Substituting equation (2) into equations (3) yields

$$\Delta X = J_x V_1 + J_y V_2 + J_z V_3$$

$$\Delta Y = J_x V_2 + J_y V_4 + J_z V_5$$

$$(4) \quad \Delta Z = J_x V_3 + J_y V_5 + J_z V_6$$

where
$$V_1 = \iiint \frac{3x^2 - R^2}{R^5} \; dxdydz$$

$$V_2 = \iiint \frac{3xy}{R^5} \; dxdydz$$

$$V_3 = \iiint \frac{3xz}{R^5} \; dxdydz$$

$$V_4 = \iiint \frac{3y^2 - R^2}{R^5} \; dxdydz$$

$$V_5 = \iiint \frac{3yz}{R^5} \; dxdydz$$

$$(5) \quad V_6 = \iiint \frac{3z^2 - R^2}{R^5} \; dxdydz$$

To evaluate V_1 thru V_6 , a double integration was done analytically in the xy plane and a numerical integration in the z direction.

The following is a discussion of the evaluation of V_1 through V_6 . Q which produces the anomaly is cut up into a discrete number of depth contours, see Fig. 19. A given depth contour is approximated by a polygon, i.e. KLMNTDFK. The anomaly is calculated at the point $P(0,0,0)$ and $P(0,0,z)$ is the point in Q that lies in the plane KLMNTDFK. Then the surface part of the integrals are obtained by analytically integrating equation (5) at the given depth, the value of z of the polygon, yielding

$$S_1 = \iint \frac{3x^2 - R^2}{R^5} \, dxdy = -\sum_i \frac{\cos^2\theta_i}{z^2 + P_i^2} \left(\frac{g_i y_{i+1} - z^2 \tan\theta_i}{R_{i+1}} \right.$$

$$\left. - \frac{g_i y_i - z^2 \tan\theta_i}{R_i} \right)$$

$$S_2 = \iint \frac{3xy \, dxdy}{R^5} = \sum_i \frac{\cos^2\theta_i}{z^2 + P_i^2} \left(\frac{g_i y_{i+1} \tan\theta_i + g_i^2 + z^2}{R_{i+1}} \right.$$

$$\left. - \frac{g_i y_i \tan\theta_i + g_i^2 + z^2}{R_i} \right)$$
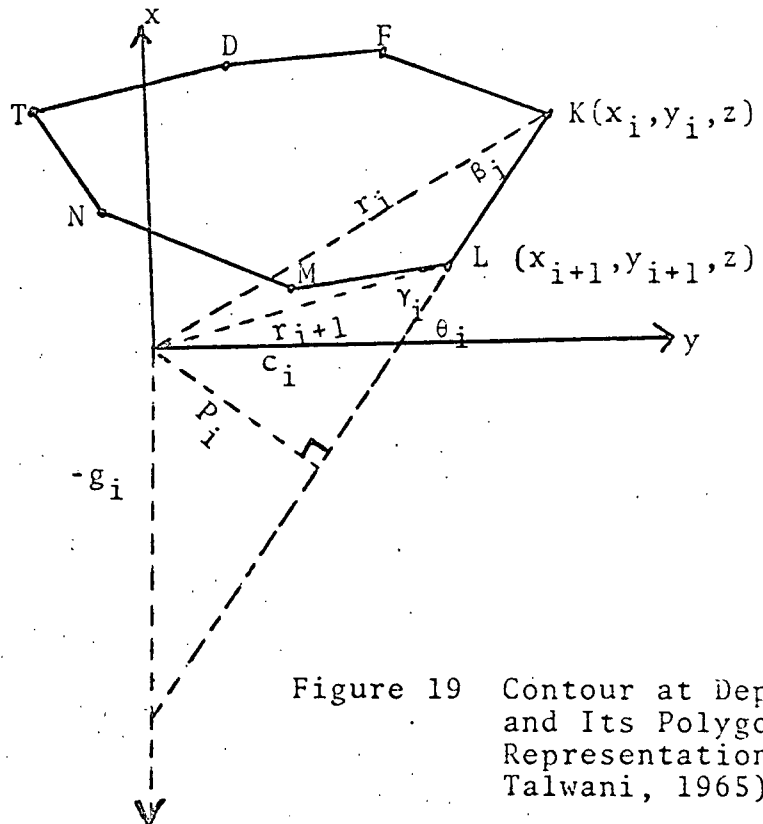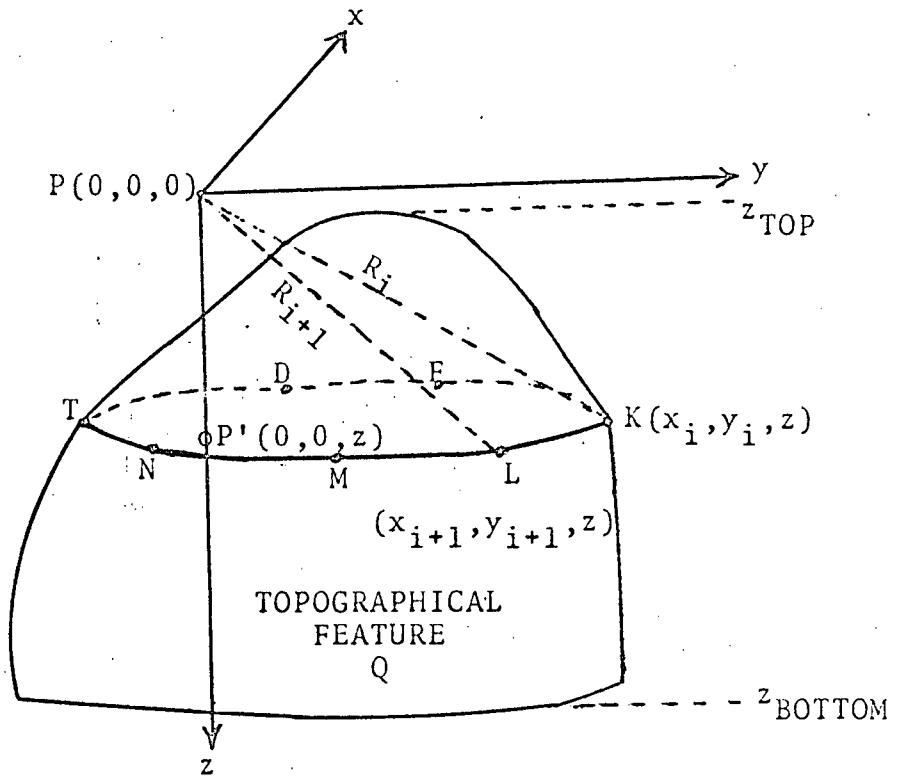
Figure 19 Contour at Depth z and Its Polygon Representation (after Talwani, 1965).

$$S_3 = \iint \frac{3xz\,dx\,dy}{R^5} = -\sum_i \frac{z^2\cos^2\theta_i}{z^2+P_i^2}\left(\frac{y_{i+1}\sec^2\theta_i+g_i\tan\theta_i}{R_{i+1}}\right.$$

$$\left.-\frac{y_i\sec^2\theta_i+g_i\tan\theta_i}{R_i}\right)$$

$$S_4 = \iint \frac{(3y^2-R^2)dx\,dy}{R^5} = \sum_i \frac{\sin^2\theta_i}{z^2+P_i^2}\left(\frac{c_ix_{i+1}-z^2\cot\theta_i}{R_{i+1}}\right.$$

$$\left.-\frac{c_ix_i-z^2\cot\theta_i}{R_i}\right)$$

$$S_5 = \iint \frac{3yz}{R^5}\,dx\,dy = \sum_i \frac{z\sin^2\theta_i}{z^2+P_i^2}\left(\frac{x_{i+1}\operatorname{cosec}^2\theta_i+c_i\cot\theta_i}{R_{i+1}}\right.$$

$$\left.-\frac{x_i\operatorname{cosec}^2\theta_i+c_i\cot\theta_i}{R_i}\right)$$

(6) $$S_6 = \iint \frac{3z^2-R^2}{R^5}\,dx\,dy = -\sum_i \frac{P_i}{z^2+P_i^2}\left(\frac{r_{i+1}\cos\gamma_i}{R_{i+1}}\right.$$

$$\left.-\frac{r_i\cos\beta_i}{R_i}\right)$$

where θ_i , β_i , γ_i , r_i , r_{i+1} , R_i , R_{i+1} , P_i , g_i , and c_i' are all defined in Fig. 19. The trigonometric functions and the lengths - c_i, P_i, g_i, r_i,

r_{i+1}, R_i, and R_{i+1} - can all be expressed in terms x_i, y_i-K- and x_{i+1}, y_{i+1}-L. The above integrals are evaluated for all the polygons. To find V_i , $\int S_i dz$ is integrated numerically where the limits, z_{top} and z_{bottom}, are defined as in Fig. 19. The integration is accomplished by fitting parabolas to successive points, values of S_i .

Shifting the origin successively to the other field points and referencing the corners of the polygon to those points, one obtains corresponding values for V_1 thru V_6 . If the values of J_x , J_y , and J_z are known, then the values of ΔX , ΔY , and ΔZ are attained by substituting the values of V_1 thru V_6 in equation (4). Assuming the anomaly to be small compared to the undisturbed field of the earth then the total field can be assumed to be in the same direction as the undisturbed field. Therefore ΔT , the total anomaly, is given by the sum of the projections of ΔX , ΔY , and ΔZ in the direction of the undisturbed field. Thus the following is obtained

(7) $\Delta T = \Delta X \cos D \cos I + \Delta y \sin D \cos I + \Delta Z \sin I$

where D is the declination and I the inclination of the earth's magnetic field. To get ΔT in terms of J_x , J_y , and J_z , substitute equation (4) into equation (7):

$$\Delta T = J_x(V_1 \cos D \cos I + V_2 \sin D \cos I + V_3 \sin I)$$

$$+ J_y(V_2 \cos D \cos I + V_4 \sin D \cos I + V_5 \sin I)$$

$$(8) \qquad + J_z(V_3 \cos D \cos I + V_5 \sin D \cos I + V_6 \sin I) \quad .$$

From equation (8) one notes that the coefficients of J_x, J_y, and J_z depend only on the geometry of the topographical feature and the direction of the earth's magnetic field. If the coefficients are determined for a given feature and for a given direction of the earth's magnetic field, then the total intensity anomaly for different magnitudes and directions of the total magnetization vector is obtained by multiplication. Conversely, if the total intensity anomaly is known from a survey, one can obtain a least squares solution of J_x, J_y, and J_z, and hence determine a best fit model using the least squares solution of $\vec{J}$.

VIII-3 Applications of the Model

In applying Talwani's program*, two systems of polygons were used: See Figures 20 and 21. Table VII gives the results of the model studies. In the Table I,

---

*A Fortran II version of the program was obtained from Talwani.

.1

1.0

1.6
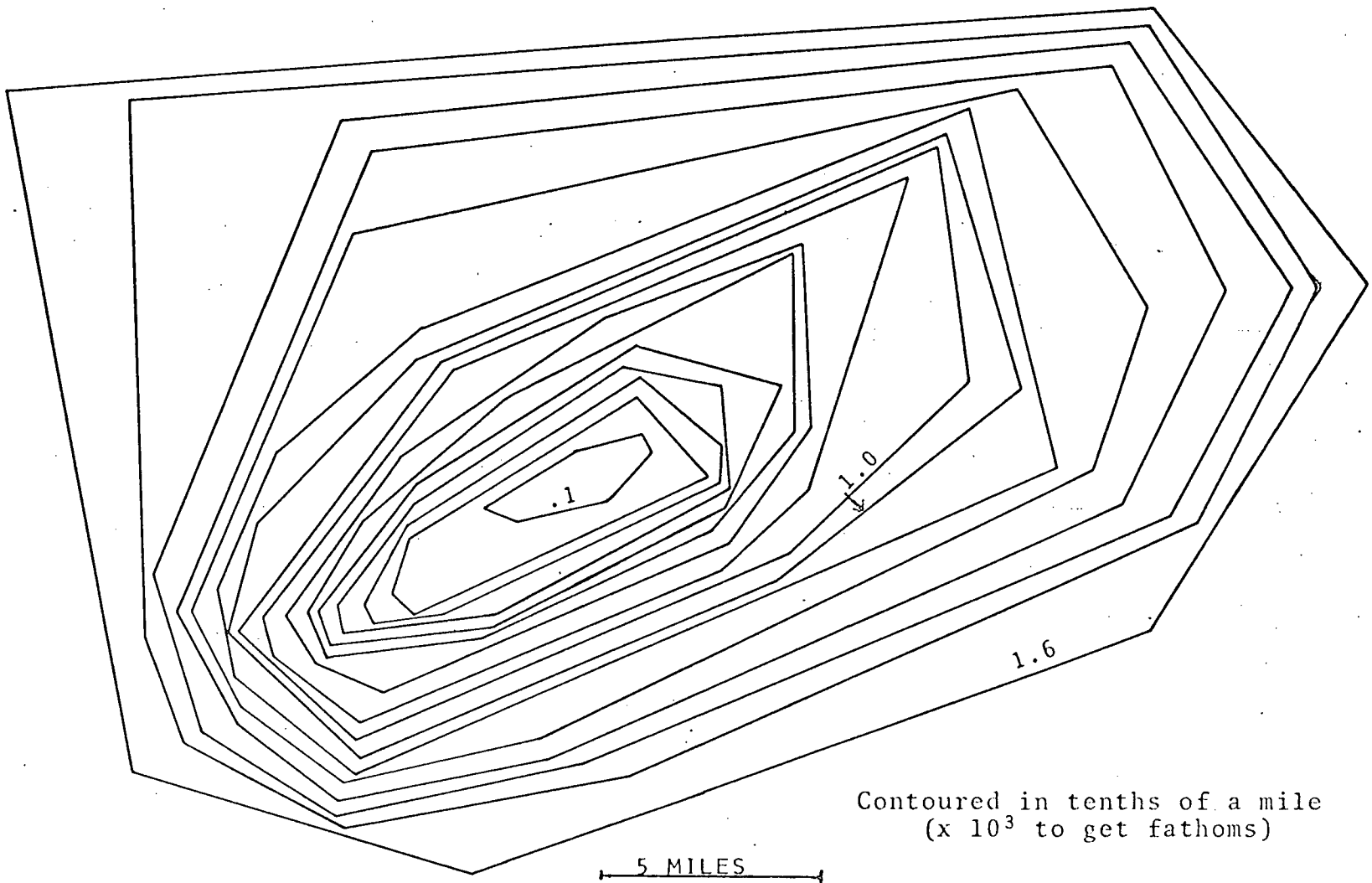
Contoured in tenths of a mile
(x 10³ to get fathoms)

5 MILES

Figure 20 Polygon System A
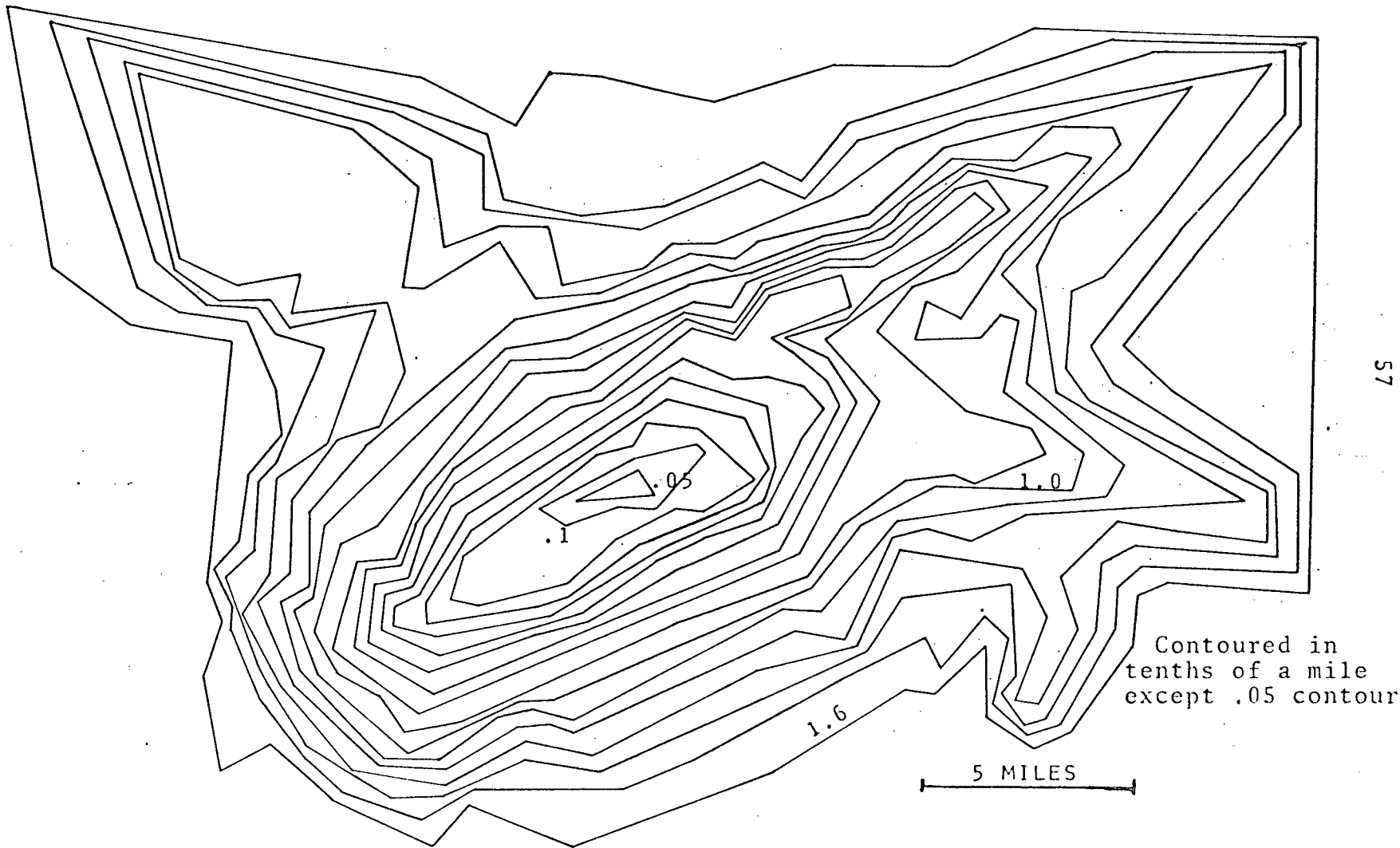
Figure 21   Polygon System B

TABLE VII

MODEL RESULTS

Model No.	Polygon System Fig	Model Characteristics	Mean Difference (gammas)	D	I	A*	B**
1	Fig. 20	Anomaly due to induction only	314.2	26.5°W	71.5°N		
2	Fig. 21 no 50 fathom contour	Anomaly due to induction only	313.2	26.5°W	71.5°N		
3	Fig. 20	Anomaly due to remanence plus induction, $\vec{J}$ assumed	605	26.5°W	71.5°N	71.5	180.0
4	Fig. 21 no 50 fathom contour	Anomaly due to remanence plus induction, $\vec{J}$ assumed	597.5	26.5°W	71.5°N	71.5	180.0
5	Fig. 20	Anomaly due to remanence plus induction (best fit $\vec{J}$)	302.7	26.5°W	71.5°N	-47.7	-2.8
6	Fig. 21 no 50 fathom contour	Anomaly due to remanence plus induction (best fit $\vec{J}$)	304.4	26.5°W	71.5°N	-33.4	41.5
7	Fig. 21	Anomaly due to remanence plus induction (best fit $\vec{J}$)	304.7	26.5°W	71.5°N	-24.6	44.6

*A is positive if measured down from the horizontal to the intensity of magnetization vector, J.

**B is positive if measured clockwise from North to the horizontal projection of the magnetization vector.

58

D, A, and B are respectively the earth's magnetic inclina-
tion - at Bowie Seamount, the earth's magnetic declination,
the inclination of $\vec{J}$ - the intensity of magnetization due
to remanence and induction, and the declination of $\vec{J}$. $\vec{J}$ is
either assumed or the calculated least squares value.
The term mean difference is merely the mean absolute dif-
ference between the observed and the calculated anomalies.

It is readily apparent that none of the models
have a low mean difference; the best fit models give values
approximately one third the value of the total magnetic
anomaly shown in Fig. 17. This was to be expected for
the assumed uniform intensity of magnetization did not
conform to the asymmetric observed anomaly. Thus the model
studies imply that Bowie Seamount is not uniformly mag-
netized.

A contour plot of a best fit calculated anomaly,
Model 7, is shown in Fig. 22. The calculated magnetic
anomaly reflects the approximate symmetry of the topography
and is in contrast with the observed anomaly. This dif-
ference is directly related to the assumption of uniform
magnetization. Fig. 23 is the contour plot of the observed
minus the calculated anomaly, i.e. the residual anomaly.
As one sees it does not significantly change the observed
anomaly.

Figure 22
CALCULATED ANOMALLY
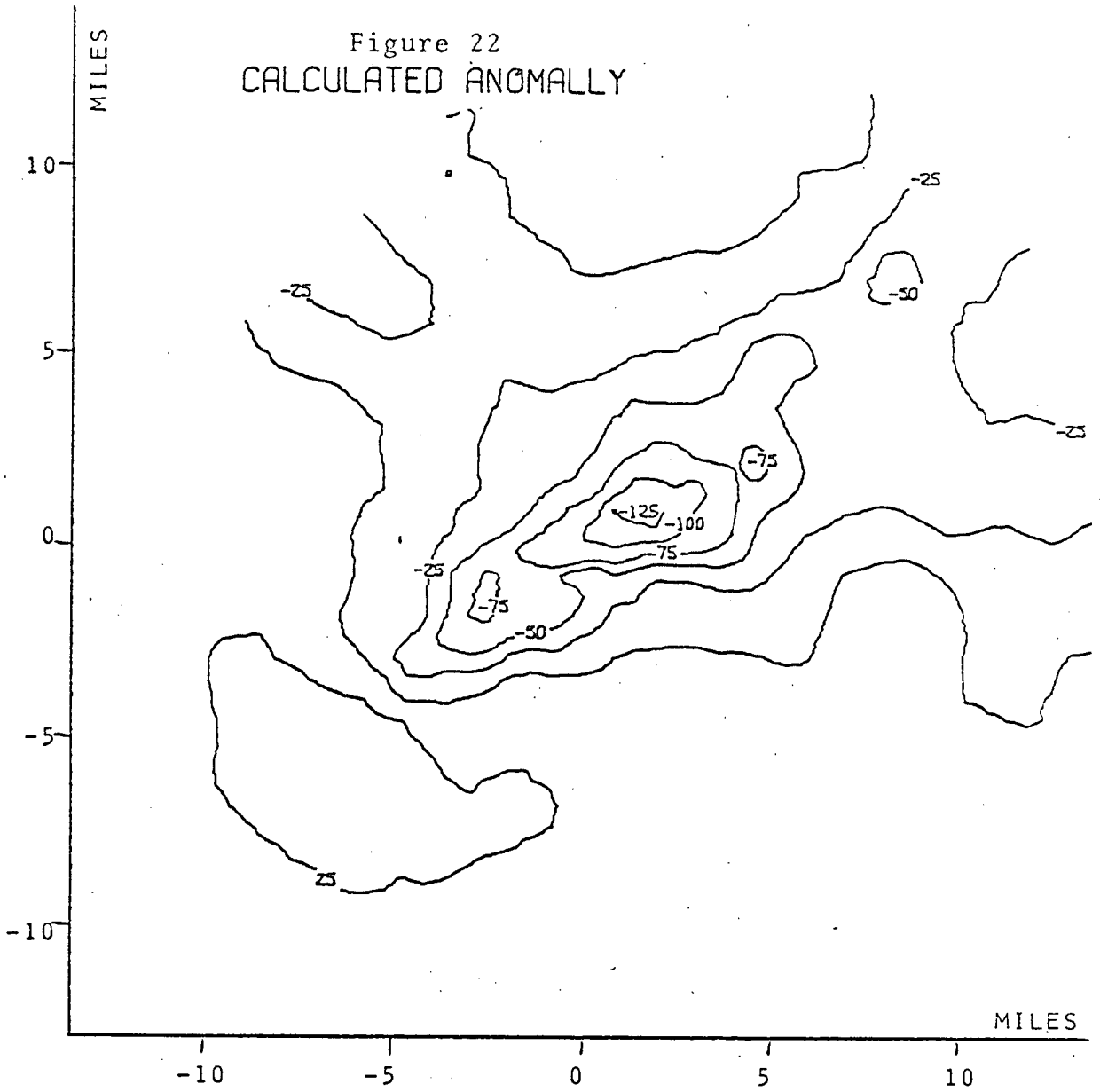
Figure 23
RESIDUAL ANOMALY
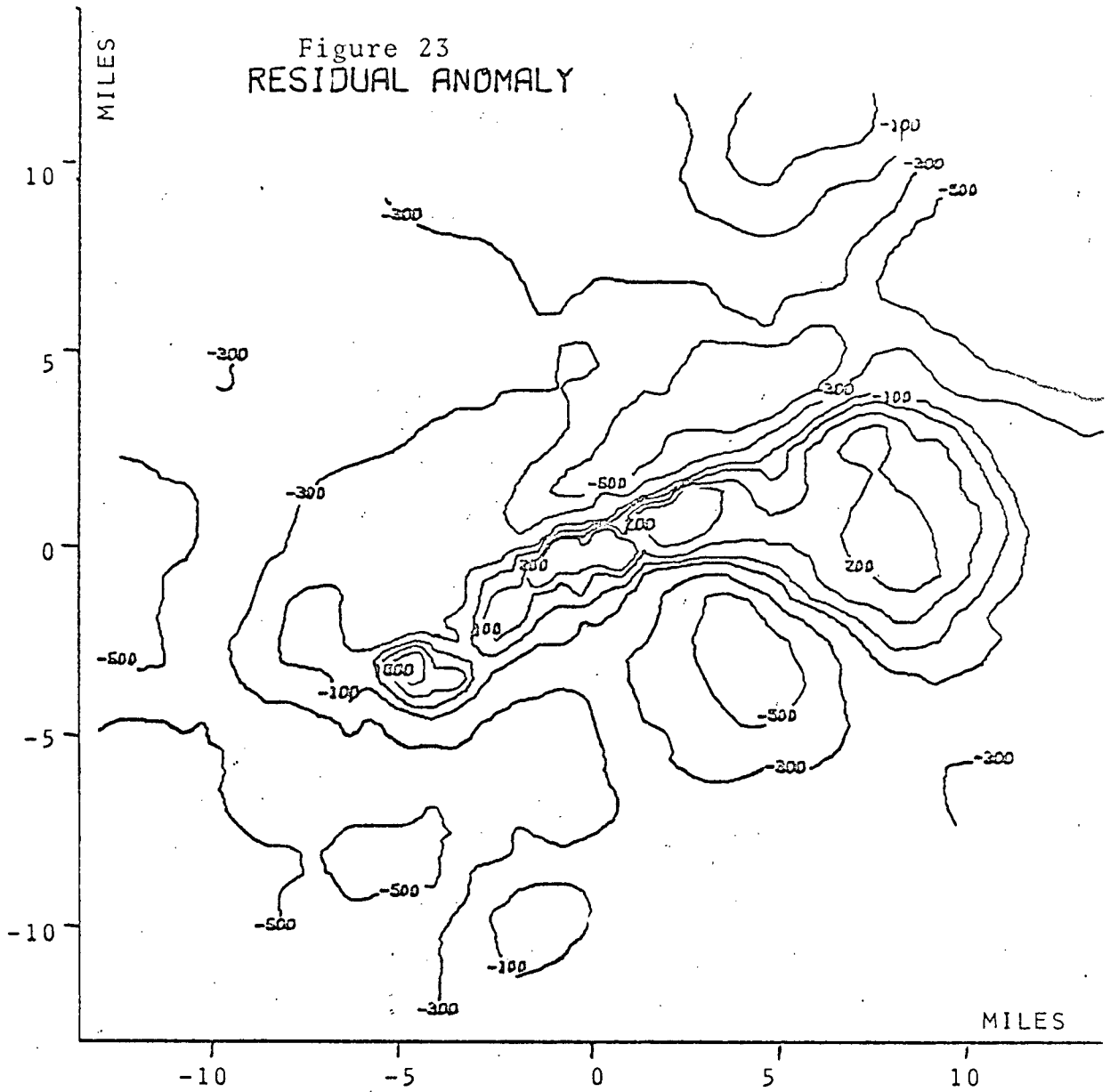
In contrast to my results the reader may be interested in an application of Talwani's program that gave a closer fit. Schimke and Bufe (1968) were able to get models for the Chautauqua Seamount ($22°11'N$, $162°34.5'W$) that had mean differences of the order of 25 gammas. This implied that the Chautauqua Seamount can be usefully represented by a model assuming uniform intensity of magnetization.

CHAPTER IX

CONCLUSIONS

It follows from Chapter VIII that the data of
the total magnetic field yields only one strong statement:
If the regional has been calculated to a sufficient degree
- a plane - Bowie Seamount cannot usefully be represented
by a model assuming a uniform intensity of magnetization.
There are at least two clear possibilities. First, the
oscillations - Fig. 5 - of the magnetic field observed on
approaching the seamount have their origin located under
the abyssal plain. Consequently this might be the cause
of the asymmetry of the magnetic field anomaly. Never-
theless, from Fig. 5 one would predict that Bowie Seamount
should have a positive magnetic field anomaly and yet
one observes a basically negative anomaly. This implies
that the seamount is primarily reversely magnetized.
Second, if one assumes that the calculated regional is
reasonable, topographical fluctuations cause a good por-
tion of the oscillations seen in Fig. 5, then Bowie Seamount
must have a very non-uniform intensity of magnetization.

Let us look at some of the major pieces of evi-
dences for saying that part of the seamount has resulted
from a flow of normally magnetized lava. First, most of
the seamount is reversely magnetized. Second, Figures 17
and 23 illustrate a sizeable yet rather local positive
anomaly in the central and the eastern part of the seamount.

Third, on the basis of the detailed topographical map - Fig. 10 - it was stated in Chapter IV that there might have been a recent lava flow in the region of the positive magnetic anomaly. Fourth, a possible feeder dyke in the area of the positive anomaly was indicated in Chapter V on the basis of a non-vesicular sample, 68-7. Fifth, the age of a rock sample at station 67-14 (Fig. 13), located in the vicinity of the positive anomaly, was found to be .075 million years (+0.1 or -0.075 million years)*. This implies (see Fig. 24 which gives the time scale for geomagnetic reversals - Cox (1969)) that the rock is normally magnetized.

The conclusion of the author is that the seamount was primarily formed during a time when the earth's magnetic field was reversed, but then there was a lava flow in the region where there is a positive anomaly at a time when the earth's magnetic field was normally magnetized. Let us assume that the seamount formed in one normal and one reversed period of the earth's magnetic field. Further if one chooses a simple model of a seamount forming continuously, then Bowie Seamount was formed between .89 million years ago and the present**.

---

*Harakal, J. (1969), K-Ar methods used for dating.

**See Fig. 24. The Laschamp event has been ignored in the conclusion because it is short-lived and is not well documented. In fact, it is solely based on the reversely magnetized lavas of the Laschamp Volcanic Cone in France.

| K-AR AGE (M.Y.) (million years)	NORMAL DATA	REVERSED DATA	FIELD NORMAL	FIELD REVERSED	AGES OF BOUNDARIES (million years)	POLARITY EVENTS	POLARITY EPOCH
					0.02	LASCHAMP EVENT	BRUNHES NORMAL EPOCH
0.5					0.03		
					0.69		
					0.89	JARAMILLO EVENT	MATUYAMA REVERSED EPOCH
1.0					0.95		
1.5					1.61		
					1.63	GILSÁ EVENT	
					1.64		
					1.79		
					1.95	OLDUVAI EVENTS	
2.0					1.98		
					2.11		
					2.13		
2.5					2.43		
					2.80	KAENA EVENT	GAUSS NORMAL EPOCH
					2.90		
3.0					2.94	MAMMOTH EVENT	
					3.06		
					3.32		
3.5					3.70	COCHITI EVENT	GILBERT REVERSED EPOCH
					3.92		
4.0					4.05	NUNIVAK EVENT	
					4.25		
					4.38		
4.5					4.50		

Figure 24

Magnetic Reversals
(from Cox 1969)

BIBLIOGRAPHY

Bassinger, B.G., Marine Magnetic Study in the Northeast Chukchi Sea, *J. Geophys. Res.*, 73, 683-687, 1968.

Blackett, P.M.S., Lectures on Rock Magnetism, Jerusalem Weizmann Science Press of Israel, 1956.

Budinger, Thomas F. and Betty J. Enbysk, Department of Oceanography, University of Washington, Technical Report No. 60, Cobb Seamount, A Deep-Sea Feature Off the Washington Coast, Office of Naval Research Ref. 59-6, 1960.

Bullard, E.C., The Removal of Trend from Magnetic Surveys, *Earth Planet. Sci. Lett.*, 2, No. 4, 293-300, 1967.

Coulthard, W.J., XPAND, A Preliminary Write Up, University of British Columbia, Computing Center, 1968.

Cox, Allan, Geomagnetic Reversals, *Science*, 163, 237-245, 1969.

Curray, Joseph R., Late Quaternary History, Continental Shelves of the United States, The Quaternary of the United States, Princeton University Press, 723-735, 1965.

Doell, Richard R. and G. Brent Dalrymple, Geomagnetic Polarity Epochs: A New Polarity Event and the Age of the Brunches-Matuyama Boundary, *Science*, 152, 1060-1061, 1966.

Doell, Richard R., G. Brent Dalrymple, and Allan Cox, Geomagnetic Polarity Epochs: Sierra Nevada Data 3, *J. Geophys. Res.*, 71, No. 2, 531-541, 1966.

Gay Jr., S. Parker, Standard Curves for Magnetic Anomalies over Long Horizontal Cylinders, *Geophysics*, XXX, No. 5, 818-828, 1965.

Grossling, Bernado F., The Internal Magnetization of Seamounts and Its Computer Calculation, Geological Survey, Professional Paper 554-F, United States Government Printing Office, 1967.

Harakal, J., Personal communication, Department of Geology, University of British Columbia, 1969.

Herzer, R. Unpublished M.Sc. thesis, Department of Geology, University of British Columbia, 1969.

Irving, E., *Paleomagnetism and Its Applications to Geological and Geophysical Problems*, John Wiley and Sons, 1964.

Irving, E., L. Molyneux, and S.K. Runcorn, The Analysis of Remnent Intensities and Susceptibilities of Rocks, *Geophys. J. R. astr. Soc.*, 10, 451-464, 1966.

Irving, E., Measurement of Polarity in Oceanic Basalt, *Can. J. Earth Sci.*, 5, No. 5, 1319-1321, 1968.

Nagata, Takesi, *Rock Magnetism*, Maruzen Company Ltd., 1961.

Prindle, Robert O., Ship-Towed Magnetics in Petroleum Exploration, Quantum Electronics Division, Varian Associates, 1967.

Raff, Arthur D., Boundaries of an Area of Very Long Magnetic Anomalies in the Northeast Pacific, *J. Geophys. Res.*, 71, No. 10, 2631-2636, 1966.

Raff, A.D. and R.G. Mason, Magnetic Survey Off the West Coast of North America 40°N Latitude to 52°N Latitude, *Bull. Geol. Soc. Am.*, 72, 1267-1270, 1961.

Reford, M.S., Airborne Magnetometer Survey for Petroleum Exploration, Canadian Aero-Service Limited, 1964.

Reitz, John R. and Frederick J. Milford, *Foundation of Electromagnetic Theory*, Addison-Wesley Publishing Co. Inc., 1962.

Richards, M.L., V. Vacquier, and G.D. Van Voorhis, Calculation of the Magnetization of Uplifts from Combining Topographic and Magnetic Surveys, *Geophysics*, XXXII, No. 4, 678-706, 1967.

Schimke, Gerald R. and Charles G. Bufe, Geophysical Description of a Pacific Ocean Seamount, *J. Geophys. Res.*, 73, No. 2, 559-569, 1968.

Talwani, Manik, Computation with the Help of a Digital Computer of Magnetic Anomalies Caused by Bodies of Arbitrary Shape, *Geophysics*, XXX, No. 5, 797-817, 1965.

Varian Associates, Quantum Electronics Division, Proton
    Magnetometer, V-4937 Data Sheet.

Vine, F.J. and R.F. Macnob, A Program for Fitting the
    Magnetic Effect of a Three Dimensional Structure
    to an Observed Anomaly by Calculating the Re-
    quired Magnetization Vector, BIO Computer Note
    67-7-C, Bedford Institute of Oceanography.